



# Integrated Multi-omics Investigations Reveal the Key Role of Synergistic Microbial Networks in Removing Plasticizer Di-(2-Ethylhexyl) Phthalate from Estuarine Sediments

Sean Ting-Shyang Wei,<sup>a</sup> Yi-Lung Chen,<sup>b</sup> Yu-Wei Wu,<sup>c</sup> Tien-Yu Wu,<sup>a</sup> Yi-Li Lai,<sup>a</sup> Po-Hsiang Wang,<sup>d,e</sup> Wael Ismail,<sup>f</sup> Tzong-Huei Lee,<sup>g</sup> Yin-Ru Chiang<sup>a</sup>

<sup>a</sup>Biodiversity Research Center, Academia Sinica, Taipei, Taiwan

<sup>b</sup>Department of Microbiology, Soochow University, Taipei, Taiwan

<sup>c</sup>Graduate Institute of Biomedical Informatics, College of Medical Science and Technology, Taipei Medical University, Taipei, Taiwan

<sup>d</sup>Institute of Environmental Engineering, National Central University, Taoyuan, Taiwan

<sup>e</sup>Earth-Life Science Institute, Tokyo Institute of Technology, Tokyo, Japan

<sup>f</sup>Environmental Biotechnology Program, Life Sciences Department, College of Graduate Studies, Arabian Gulf University, Manama, Bahrain

<sup>g</sup>Institute of Fisheries Science, National Taiwan University, Taipei, Taiwan

**ABSTRACT** Di-(2-ethylhexyl) phthalate (DEHP) is the most widely used plasticizer worldwide, with an annual global production of more than 8 million tons. Because of its improper disposal, endocrine-disrupting DEHP often accumulates in estuarine sediments in industrialized countries at submillimolar levels, resulting in adverse effects on both ecosystems and human beings. The microbial degraders and biodegradation pathways of DEHP in O<sub>2</sub>-limited estuarine sediments remain elusive. Here, we employed an integrated meta-omics approach to identify the DEHP degradation pathway and major degraders in this ecosystem. Estuarine sediments were treated with DEHP or its derived metabolites, *o*-phthalic acid and benzoic acid. The rate of DEHP degradation in denitrifying mesocosms was two times slower than that of *o*-phthalic acid, suggesting that side chain hydrolysis of DEHP is the rate-limiting step of anaerobic DEHP degradation. On the basis of microbial community structures, functional gene expression, and metabolite profile analysis, we proposed that DEHP biodegradation in estuarine sediments is mainly achieved through synergistic networks between denitrifying proteobacteria. *Acidovorax* and *Sedimenticola* are the major degraders of DEHP side chains; the resulting *o*-phthalic acid is mainly degraded by *Aestuariibacter* through the UbiD-dependent benzoyl coenzyme A (benzoyl-CoA) pathway. We isolated and characterized *Acidovorax* sp. strain 210-6 and its extracellular hydrolase, which hydrolyzes both alkyl side chains of DEHP. Interestingly, genes encoding DEHP/mono-(2-ethylhexyl) phthalate (MEHP) hydrolase and phthaloyl-CoA decarboxylase—key enzymes for side chain hydrolysis and *o*-phthalic acid degradation, respectively—are flanked by transposases in these proteobacterial genomes, indicating that DEHP degradation capacity is likely transferred horizontally in microbial communities.

**IMPORTANCE** Xenobiotic phthalate esters (PAEs) have been produced on a considerably large scale for only 70 years. The occurrence of endocrine-disrupting di-(2-ethylhexyl) phthalate (DEHP) in environments has raised public concern, and estuarine sediments are major DEHP reservoirs. Our multi-omics analyses indicated that complete DEHP degradation in O<sub>2</sub>-limited estuarine sediments depends on synergistic microbial networks between diverse denitrifying proteobacteria and uncultured candidates. Our data also suggested that the side chain hydrolysis of DEHP, rather than *o*-phthalic acid activation, is the rate-limiting step in DEHP biodegradation within O<sub>2</sub>-limited estuarine sediments. Therefore, deciphering the bacterial ecophysiology and related biochemical mechanisms can help facilitate the practice of bioremediation in

**Citation** Wei ST-S, Chen Y-L, Wu Y-W, Wu T-Y, Lai Y-L, Wang P-H, Ismail W, Lee T-H, Chiang Y-R. 2021. Integrated multi-omics investigations reveal the key role of synergistic microbial networks in removing plasticizer di-(2-ethylhexyl) phthalate from estuarine sediments. *mSystems* 6:e00358-21. <https://doi.org/10.1128/mSystems.00358-21>.

**Editor** Yu-Liang Yang, Agricultural Biotechnology Research Center

**Ad Hoc Peer Reviewers** Shaohua Chen, Integrative Microbiology Research Centre, South China Agricultural University; Naresh Singhal, University of Auckland.

**Copyright** © 2021 Wei et al. This is an open-access article distributed under the terms of the [Creative Commons Attribution 4.0 International license](https://creativecommons.org/licenses/by/4.0/).

Address correspondence to Yin-Ru Chiang, yinru915@gate.sinica.edu.tw.

**Received** 24 March 2021

**Accepted** 23 May 2021

**Published** 8 June 2021

O<sub>2</sub>-limited environments. Furthermore, the DEHP hydrolase genes of active DEHP degraders can be used as molecular markers to monitor environmental DEHP degradation. Finally, future studies on the directed evolution of identified DEHP/mono-(2-ethylhexyl) phthalate (MEHP) hydrolase would bring a more catalytically efficient DEHP/MEHP hydrolase into practice.

**KEYWORDS** *Acidovorax*, di-(2-ethylhexyl) phthalate, anaerobic catabolic pathways, denitrifying bacteria, endocrine disruptor, metagenomics, phthalate esters

Phthalate esters (PAEs) are commonly used as plasticizers to improve the flexibility of plastics and their adhesive capacity in some aqueous products (1, 2). The annual production of PAEs had increased up to 8 million tons in 2011 (2), although the number dropped to 5.5 million tons in 2018 (3). The side chains of PAEs are composed of linear or branched aliphatic alcohols with various lengths (2, 4). Di-(2-ethylhexyl) phthalate (DEHP), also named bis(2-ethylhexyl) phthalate, is the most widely used plasticizer worldwide, accounting for approximately one-third and 80% of PAEs produced in the European Union and China, respectively (2). Because of the daily use of plastic worldwide and the easy diffusion of plastic polymers into the environment (5), PAEs can be detected almost everywhere in industrialized countries (2) as well as in polar regions (6).

The endocrine-disrupting and carcinogenic activities of PAEs in higher animals have raised substantial public concern (5, 7). For example, some studies have reported that in some fishery species, embryo maturation and oogenesis are impeded by even a low concentration of DEHP—0.1 to 0.2  $\mu\text{g/liter}$  (8, 9); the DEHP concentration in some freshwater ecosystems is up to a much higher 21  $\mu\text{g/liter}$  (2). In addition, DEHP not only affects endocrine and nervous systems but also is genotoxic to higher animals and humans. Despite that the lowest effective dose of DEHP varies depending on organs or cell types, it has been demonstrated that a DEHP concentration of 1  $\mu\text{g/ml}$  causes DNA damage in human lymphocyte cell lines, and exposure to 0.39  $\mu\text{g/ml}$  of DEHP was able to induce motility and proliferation of breast tumor cells (10).

Abiotically, DEHP can be photodegraded in surface water or the atmosphere with a degradation half-life ranging from weeks to years (11, 12). However, DEHP does not undergo photodegradation in aquatic sediments lacking sunlight exposure and O<sub>2</sub> (2). Moreover, the high hydrophobicity of DEHP (its water solubility is approximately 3 mg/liter) results in the adsorption of DEHP onto aquatic sediment particles (13), meaning that the content of DEHP is considerably higher in aquatic sediments than in surface water. For example, in South Africa, the DEHP concentration is approximately 6  $\mu\text{g/liter}$  in river water, whereas it is up to 3,660  $\mu\text{g/kg}$  in sediments in the same river (2). Moreover, the salinity of estuarine environments enhances the adsorption of DEHP onto estuarine sediments because of salt fractionation (13).

Biodegradation is the primary process through which PAEs are removed in municipal wastewater treatment plants (2). Several studies have reported aerobic microbial degradation pathways for different PAEs (4). In the aerobic pathway, DEHP is initially transformed into *o*-phthalic acid and 2-ethylhexanol through mono-(2-ethylhexyl) phthalate (MEHP) by dialkyl phthalate hydrolase and monoalkyl phthalate hydrolase (14–16) (Fig. 1). Subsequently, *o*-phthalic acid is converted to protocatechuate (3,4-dihydroxybenzoate), which is followed by ring cleavage through either the *ortho*-cleavage (by intradiol dioxygenases) or *meta*-cleavage (by extradiol dioxygenases) pathway (Fig. 1) (4, 17). In contrast, the anaerobic DEHP biodegradation pathway remains unclear. Nevertheless, the anaerobic degradation pathway of *o*-phthalic acid has recently been characterized in some denitrifying bacteria and sulfate-reducing bacteria (18–20). Briefly, *o*-phthalic acid is activated by either type III coenzyme A (CoA) transferase or ATP-dependent CoA transferase to form the highly unstable phthaloyl-CoA; this is followed by nonoxidative decarboxylation to form benzoyl-CoA by prenylated flavin mononucleotide (FMN)-dependent phthaloyl-CoA decarboxylase in the UbiD family

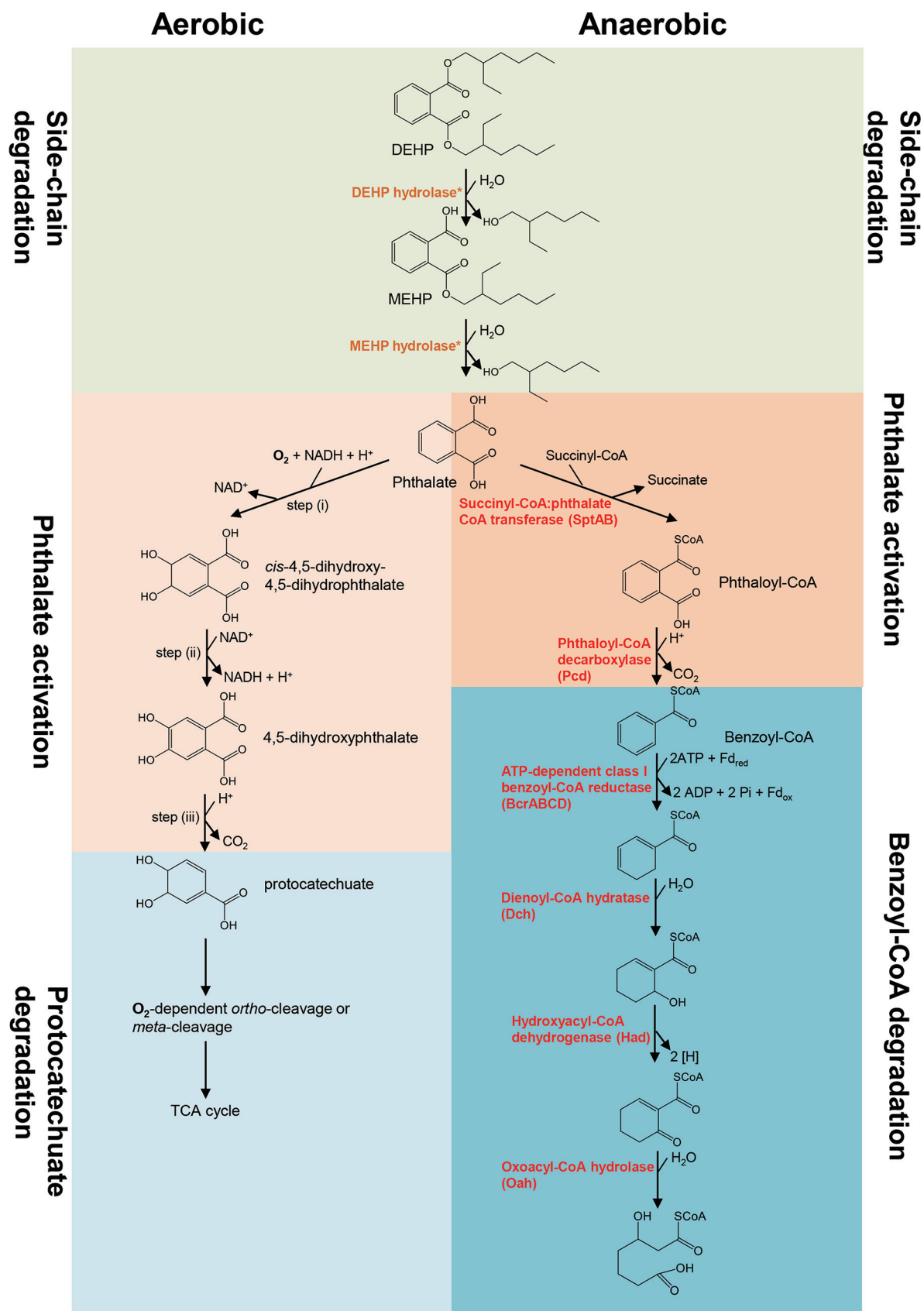


**FIG 1** Proposed microbial degradation pathways of DEHP. (Left) Simplified aerobic degradation pathway with 4,5-dihydroxyphthalate and protocatechuate as characteristic intermediates. An alternative aerobic pathway with 3,4-dihydroxyphthalate and protocatechuate as (Continued on next page)

(21). Subsequently, the core ring of benzoyl-CoA is cleaved through the well-established benzoyl-CoA degradation pathway (17, 19, 20) (Fig. 1). However, whether these *o*-phthalic acid-degrading anaerobes can degrade DEHP remains unclear.

Wetland sediments in estuaries provide essential ecosystem services (water purification and toxin trapping) for urban environments and are major reservoirs of DEHP worldwide. To identify autochthonous anaerobic DEHP microbial degraders and elucidate the underlying biochemical and molecular mechanisms, we performed mesocosm experiments by incubating Guandu estuarine sediments with DEHP under denitrifying conditions. We used ultraperformance liquid chromatography (UPLC)–high-resolution mass spectrometry (HRMS) to identify DEHP-derived metabolites. Subsequently, we adopted next-generation sequencing approaches to identify DEHP-degrading bacteria and their degradation genes. Furthermore, we isolated the DEHP-degrading *Acidovorax* sp. and purified the DEHP/MEHP hydrolase from the sediment isolate. Both culture-independent and culture-dependent results suggested that DEHP was mainly removed from the estuarine sediments through synergistic microbial degradation, and side chain hydrolysis represents a bottleneck in the DEHP degradation process.

(This article was submitted to an online preprint archive [22].)

## RESULTS

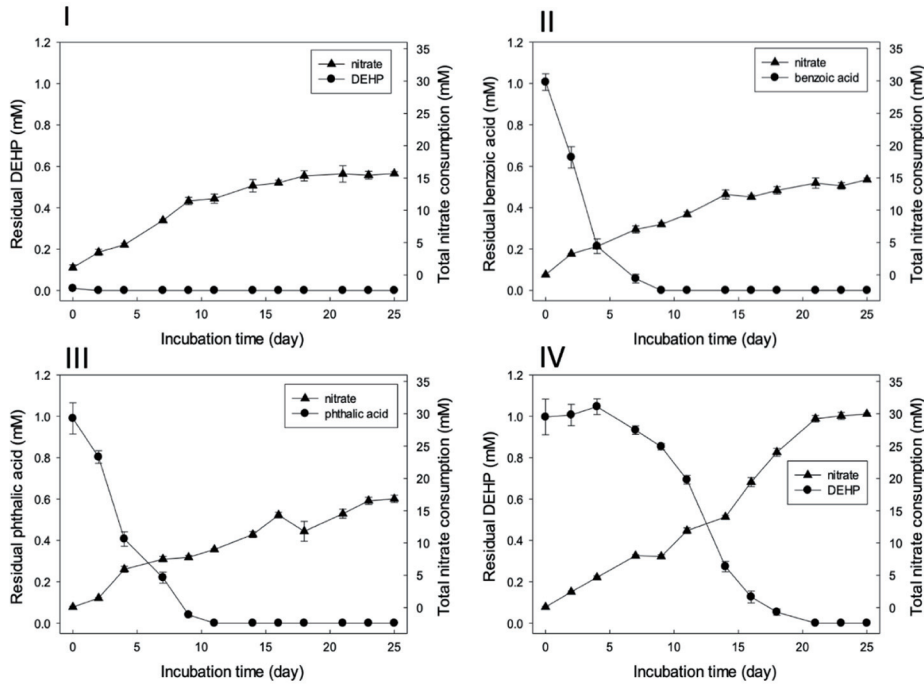
**DEHP biodegradation in denitrifying sediment mesocosms.** Sediment mesocosms (1 liter; two replicates in each treatment) composed of estuarine sediment (approximately 200 g) and river water (approximately 800 ml) were treated with sodium nitrate alone (10 mM; sediment-nitrate [SN]), nitrate (10 mM) and benzoic acid (1 mM) (sediment-benzoic acid-nitrate [SBN]), nitrate (10 mM) and *o*-phthalic acid (1 mM) (sediment-*o*-phthalic acid-nitrate [SPN]), or nitrate (10 mM) and DEHP (1 mM) (sediment-DEHP-nitrate [SDN]). Benzoic acid and *o*-phthalic acid have been proposed as crucial intermediates of the established anaerobic DEHP degradation pathway (17). The concentrations of endogenous benzoic acid, *o*-phthalic acid, and DEHP in these sediment mesocosms ranged from 0.001 to 0.01 mM, approximately 100-fold lower than those in exogenous substrates. Sediment mesocosms that received different treatments displayed discernible patterns in substrate depletion rate and total nitrate consumption. The SN1 (nitrate alone, replicate 1) mesocosm had consumed  $15.5 \pm 0.92$  mM nitrate in total after 25 days of anaerobic incubation (Fig. 2AI). In the SBN1 mesocosm, exogenous benzoic acid was largely depleted (approximately 80%) within 4 days of continuous nitrate consumption (Fig. 2AII). Approximately 80% of *o*-phthalic acid in the SPN1 mesocosm was consumed within 1 week (Fig. 2AIII). Notably, the DEHP consumption rate was lowest in the denitrifying sediment. Approximately 35% of the DEHP in SDN1 was consumed within 11 days, and the DEHP was depleted at day 21, together with a total nitrate consumption of  $29.8 \pm 0.16$  mM (Fig. 2AIV). The mesocosms in all duplicates showed similar trends in the utilization of exogenous substrates (see Fig. S1 in the supplemental material). We noted that the DEHP in SDN2 was completely degraded at day 25, with a total nitrate consumption of  $25.8 \pm 0.22$  mM (Fig. S1D).

DEHP-derived metabolites in the SDN1 samples were then identified through UPLC-atmospheric pressure chemical ionization (APCI)-HRMS (Fig. 3). We observed the production and subsequent consumption of two non-CoA thioester metabolites (MEHP and *o*-phthalic acid) (Fig. 3A). These DEHP-derived metabolites were not detected within the first week of denitrifying incubation, whereas MEHP ( $0.08 \pm 0.01$  mM) and *o*-phthalic acid ( $0.19 \pm 0.02$  mM) had temporarily accumulated after 16 days of incubation (Fig. 3B).

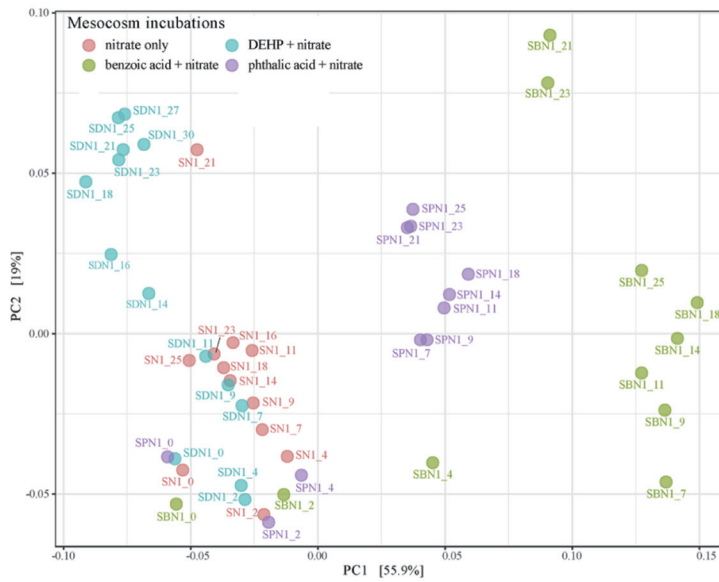
### FIG 1 Legend (Continued)

characteristic intermediates has also been identified. (Right) Proposed anaerobic degradation pathway for PAEs established in denitrifying *Aromatoleum*, *Azoarcus*, and *Thauera*. Proteins involved in this anaerobic pathway are shown in red.\*; Dialkyl phthalate and monoalkyl phthalate hydrolases were functionally characterized in aerobic *Gordonia* and anaerobic *Acidovorax* sp. strain 210-6 prior to this study. Fd, ferredoxin; TCA, tricarboxylic acid.

(A)



(B)



(C)

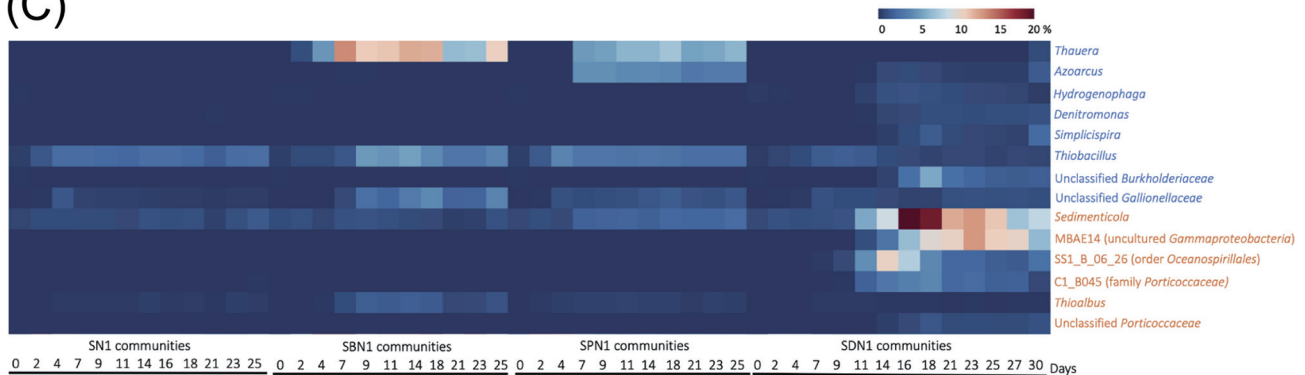


**FIG 2** Estuarine sediments treated with benzoic acid, o-phthalic acid, and DEHP in denitrifying mesocosms. (A) Substrate utilization and nitrate consumption in anoxic sediments incubated with nitrate only (I), sediments incubated with benzoic acid and nitrate (II), sediments incubated with (Continued on next page)

**Betaproteobacteria and gammaproteobacteria as key DEHP degraders in denitrifying sediment mesocosms.** In total, 5,582 operational taxonomic units (OTUs) were generated in all the sediment communities of replicate 1. PC1 (55.9% of total explained variance) and PC2 (19.0% of total explained variance) in the principal-coordinate analysis (PCoA) clearly distinguished the microbial communities among SN1, SBN1, SPN1, and SDN1. Most of the SN1 communities—together with communities from the early incubation stage (day 2 to day 4) of the SBN1, SPN1, and SDN1 mesocosms—were clustered in the lower-left corner of the coordinate, slightly distant from the sediment communities at the beginning of the experiment (incubation time of 30 min). However, communities from the middle and late incubation stages (day 9 to 30) of SBN1, SPN1, and SDN1 mesocosms were clustered separately (Fig. 2B). The results of permutational multivariate analysis of variance (PERMANOVA) revealed that the weighted UniFrac distance of overall bacterial genera in each community was significant ( $F$  value = 12.405, global  $R^2$  = 0.45823,  $P$  value < 0.001).

In the benzoic acid and *o*-phthalic acid mesocosms, we observed enrichment of the betaproteobacteria *Thauera* and *Azoarcus* (Fig. 2C); this enrichment was associated with the consumption of the substrates within 1 week (Fig. 2AII and AIII). These two bacterial genera were not enriched in the SN1 mesocosm treated with nitrate alone. In the SBN1 community, the relative abundance of *Thauera* increased from <0.1% at day 0 to 12.5% at day 7. The abundances of *Thauera* and *Azoarcus* in the SPN1 community had increased to 5.8% and 3.9%, respectively, at day 11. Although *o*-phthalic acid was identified as a major DEHP metabolite in the SDN1 mesocosm (Fig. 3), the enrichment of the aforementioned two genera was considerably less (~1%) in the SDN1 community. Instead, we observed large enrichment ( $\geq 10\%$ ) of three gammaproteobacterial genera—namely, *Sedimenticola*, MBAE14 (uncultured *Gammaproteobacteria*), and SS1\_B\_06\_26 (belonging to the order *Oceanospirillales*)—in the SDN1 community. In addition, the relative abundance of other bacteria, such as C1\_B045 (gammaproteobacterial family *Porticoccaceae*) and an unclassified *Burkholderiaceae* (*Betaproteobacteria*), increased but to a lower extent (approximately 5%) (Fig. 2C).

In the SN2, SBN2, SPN2, and SDN2 mesocosms (replicate 2), 5,708 OTUs were identified. The results of PCoA and temporal changes in the relative abundance of the aforementioned genera were similar to those observed for replicate 1 (see Fig. S2 and S3).

**Putative carboxylesterase and  $\beta$ -oxidation genes involved in alkyl side chain degradation in the DEHP-treated mesocosms.** In differential gene expression (DGE) analysis, only 1,800 genes were observed to be upregulated in the SPN sediments, whereas up to 40,867 genes were upregulated in the SDN mesocosms (see Fig. S4). In the SDN mesocosms, 205 alpha/beta hydrolase and esterase genes belonging to the carboxylesterase superfamily were annotated on the basis of eggNOG annotation in the DEHP-treated sediments. Only six genes—k141\_3815848\_2, k141\_2812817\_2, k141\_4060503\_4, k141\_138169\_2, k141\_2938615\_2, and k141\_853245\_1—were similar to the functionally characterized hydrolase gene encoding [NCU65476](#) of the denitrifying *Acidovorax* sp. strain 210-6 according to the hidden Markov model (HMM) search (the isolation and characterization of strain 210-6 and its DEHP/MEHP hydrolase are described later). Proteins encoded by these genes belonged to the IPR029058 carboxylesterase superfamily, and signal peptides were present on the proteins of k141\_3815848\_2, k141\_2812817\_2, k141\_4060503\_4, and k141\_853245\_1 (Table 1). After examining the binned genomes recovered from metagenomes (described in the next section), these genes were distributed in Bin6, Bin13, Bin14, Bin18, and Bin44, and their taxonomic affiliations were *Acidovorax* sp.

## FIG 2 Legend (Continued)

*o*-phthalic acid and nitrate (III), and sediments incubated with DEHP and nitrate (IV). The values are shown as means from three independent measurements with standard deviations for mesocosm replicate 1. (B) PCoA for the determination of similarities between the bacterial communities of mesocosm replicate 1 based on UniFrac distance matrix data (genus level) obtained from the sediment incubated with nitrate (SN1), sediment with benzoic acid and nitrate (SBN1), sediment with *o*-phthalic acid and nitrate (SPN1), and sediment with DEHP and nitrate (SDN1). (C) Relative abundance changes of genera of *Betaproteobacteria* (blue) and *Gammaproteobacteria* (orange) from sediment incubated with nitrate (SN1), with benzoic acid and nitrate (SBN1), with *o*-phthalic acid and nitrate (SPN1), and with DEHP and nitrate (SDN1) in mesocosm replicate 1. SS1\_B\_06\_26 belongs to the order *Oceanospirillales*, and C1\_B045 belongs to the family *Porticoccaceae*.

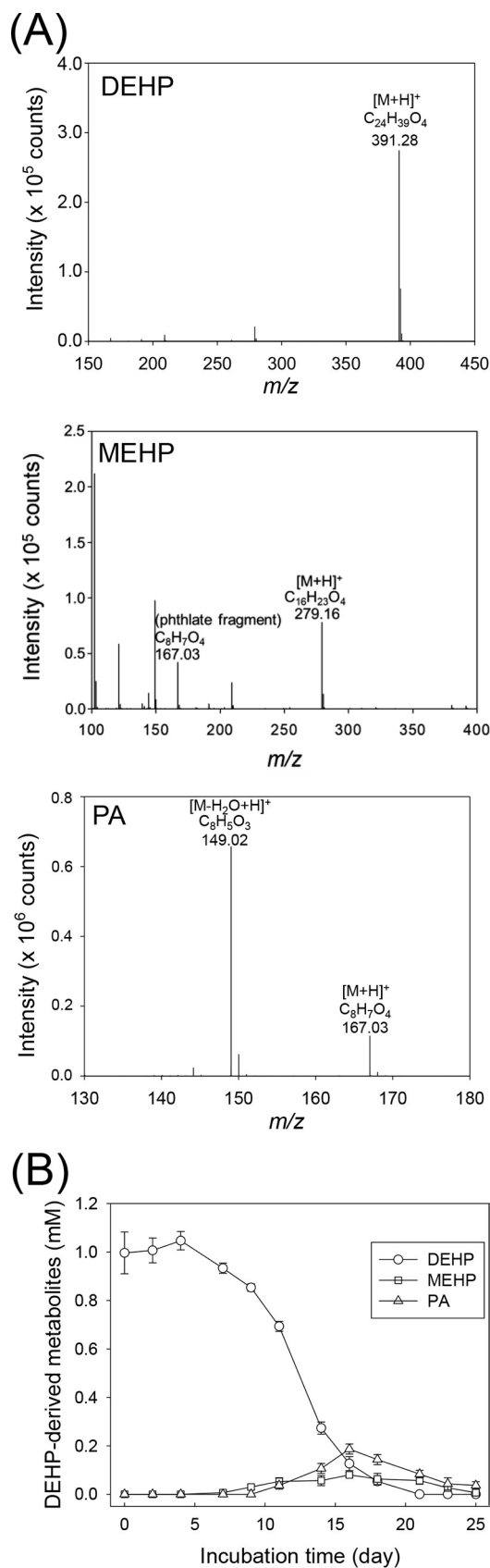


**FIG 3** Metabolite profile analysis of DEHP-treated sediment mesocosm (replicate 1). (A) APCI-HRMS spectra of non-CoA metabolites detected in the mesocosm. PA, *o*-phthalic acid. (B) Time course of DEHP (Continued on next page)

**TABLE 1** Hydrolases potentially involved in the degradation of DEHP alkyl side chain in DEHP-treated sediments

Gene or accession no.	Genome	InterPro superfamily	Signal peptide (aa) <sup>a</sup>
k141_3815848_2	<i>Acidovorax</i> Bin6	IPR029058 AB_hydrolase	Secretory signal peptide (1–25)
k141_2812817_2	<i>Burkholderiales</i> Bin13	IPR029058 AB_hydrolase	Secretory signal peptide (1–37)
k141_4060503_4	<i>Burkholderiales</i> Bin13	IPR029058 AB_hydrolase	Secretory signal peptide (1–23)
k141_138169_2	<i>Sedimenticola</i> Bin14	IPR029058 AB_hydrolase	ND
k141_2938615_2	<i>Ketobacter</i> Bin18	IPR029058 AB_hydrolase	ND
k141_853245_1	<i>Aestuariibacter</i> Bin44	IPR029058 AB_hydrolase	lipoprotein signal peptide (1–20)
OGB81769.1 <sup>b</sup>	<i>Burkholderiales bacterium</i>	IPR029058 AB_hydrolase	Secretory signal peptide (1–23)
WP_132980767.1 <sup>b</sup>	<i>Pigmentiphaga</i> sp. D-2	IPR029058 AB_hydrolase	Secretory signal peptide (1–23)
WP_130355623.1 <sup>b</sup>	<i>Pigmentiphaga kullae</i>	IPR029058 AB_hydrolase	Secretory signal peptide (1–23)

<sup>a</sup>aa, amino acid position of the signal peptide; ND, not determined.

<sup>b</sup>Proteins displayed >70% amino acid identity to DEHP/MEHP hydrolase (NCU65476) of *Acidovorax* sp. strain 210-6. Details may be found in "Phylogenetic analysis of phthaloyl-CoA decarboxylases and DEHP/MEHP hydrolases."

HMWF018 (*Betaproteobacteria*), *Burkholderiales bacterium* 68-12 (*Betaproteobacteria*), *Sedimenticola selenatireducens* (*Gammaproteobacteria*), *Ketobacter alkanivorans* (*Gammaproteobacteria* *Ocea-nospirillales*), and *Aestuariibacter aggregatus* (*Gammaproteobacteria*), respectively (Table 2). In addition, differentially expressed  $\beta$ -oxidation genes were identified in these binned genomes (Fig. 4A). Bin13, Bin14, and Bin18 contained genes involved in nitrate and nitrite reduction, chemotaxis, and flagellar synthesis (see Data Set S1); some of them were differentially expressed (Table 3). Differentially expressed hydrolase or esterase genes were not identified in the SPN mesocosms.

**Binned genomes with complete *o*-phthalic acid degradation capacity in the DEHP-treated mesocosms.** In the SDN mesocosms, 23 genes belonging to the UbiD-like decarboxylase family were upregulated. According to blastp results, only eight UbiD homologs identified in eight contigs share high amino acid sequence identity (AAI; 74% to 85%) to phthaloyl-CoA decarboxylase of *Aromatoleum aromaticum* EbN1 (DSM 19081), *Azoarcus toluclasticus* ATCC 700605, and *Thauera chlorobenzoica* 3CB-1 (DSM 18012) (Data Set S1). Furthermore, we discovered genes annotated as flavin prenyltransferase (UbiX) (23), CoA-transferase, TRAP transporter, and transposase in some of these contigs (Data Set S1); however, none of these genes were differentially expressed in the SDN mesocosms.

We selected binned genomes containing the phthaloyl-CoA decarboxylase gene to determine whether they could anaerobically degrade *o*-phthalic acid. Up to 394 binned genomes were generated by MaxBin 2.0, but 115,543 contigs were unbinned. We observed that three contigs with phthaloyl-CoA decarboxylase genes were binned into Bin44, whereas in other binned genomes—Bin54, Bin60, and Bin116—only a single contig with the phthaloyl-CoA decarboxylase gene was binned (Fig. 4B). However, two contigs—K141\_1830739 and K141\_260687—with this gene were not binned (Data Set S1).

Two genes involved in *o*-phthalic acid uptake were also identified in these binned genomes (except for Bin116) and two unbinned contigs. Moreover, crucial genetic components for anaerobic benzoyl-CoA degradation, including benzoyl-CoA reductase (*brcABCD*), dienoyl-CoA hydratase (*dch*), hydroxyacyl-CoA dehydrogenase (*had*), and oxoacyl-CoA hydrolase (*oah*), were identified in Bin44, Bin54, and Bin60; in Bin116, only one gene encoding benzoyl-CoA reductase subunit A (*brcA*) was recovered (Fig. 4B and Data Set S1). In addition, we noted that most of the genes related to nitrate reduction, chemotaxis, and flagellar synthesis were differentially expressed in Bin44, Bin54, and Bin60 (Table 3 and Data Set S1).

The closest taxonomic affiliations of Bin44, Bin54, Bin60, and Bin116 were *Aestuariibacter aggregatus* (*Gammaproteobacteria*), *Azoarcus communis* (*Betaproteobacteria*), *Aestuariibacter aggregatus*, and unclassified *Gammaproteobacteria bacterium* BRH\_c0, respectively. The

### FIG 3 Legend (Continued)

consumption and production of DEHP-derived metabolites in the sediment mesocosm. Quantification of the DEHP metabolites was based on pseudomolecular ( $[M+H]^+$ ) ion counts corresponding to individual compounds by using UPLC-HRMS. Data shown are the means  $\pm$  standard deviations from three experimental measurements.



**TABLE 2** Features and quality of binned genomes that had partial or complete capacity to degrade DEHP

Bin	Total length (bp)	No. of contigs	$N_{50}$	GC (%)	Taxonomy	AAI to closest species (%)	CheckM completeness (%)	CheckM contamination (%)	Degradation capacity
Bin44	1,715,874	330	10,375	48.15	Gammaproteobacteria	<i>Aestuariibacter aggregatus</i> (84.1)	46.55	26.8	Alkyl side chain, phthalic acid
Bin6	251,465	125	1,929	63.07	Betaproteobacteria	<i>Acidovorax</i> sp. HMWF018 (97.12)	4.02	0	Alkyl side chain
Bin13	370,293	60	11,924	62.49	Betaproteobacteria	<i>Burkholderiales bacterium</i> 68-12 (84.61)	25.86	6.43	Alkyl side chain
Bin14	472,849	30	25,611	58.34	Gammaproteobacteria	<i>Sedimenticola selenatireducens</i> (85.94)	15.99	0	Alkyl side chain
Bin18	843,089	125	18,585	57.57	Gammaproteobacteria	<i>Ketobacter alkanivorans</i> (65.59)	24.29	6.9	Alkyl side chain
Bin54	1,716,048	347	8,133	64.99	Betaproteobacteria	<i>Azoarcus communis</i> (74.7)	66.61	26.03	Phthalic acid
Bin60	5,123,840	411	31,029	47.30	Gammaproteobacteria	<i>Aestuariibacter aggregatus</i> (85.9)	93.65	35.95	Phthalic acid
Bin116	443,991	236	1,808	56.74	Gammaproteobacteria	<i>Gammaproteobacteria bacterium</i> BRH_c0 (84.1)	3.82	0.35	Phthalic acid

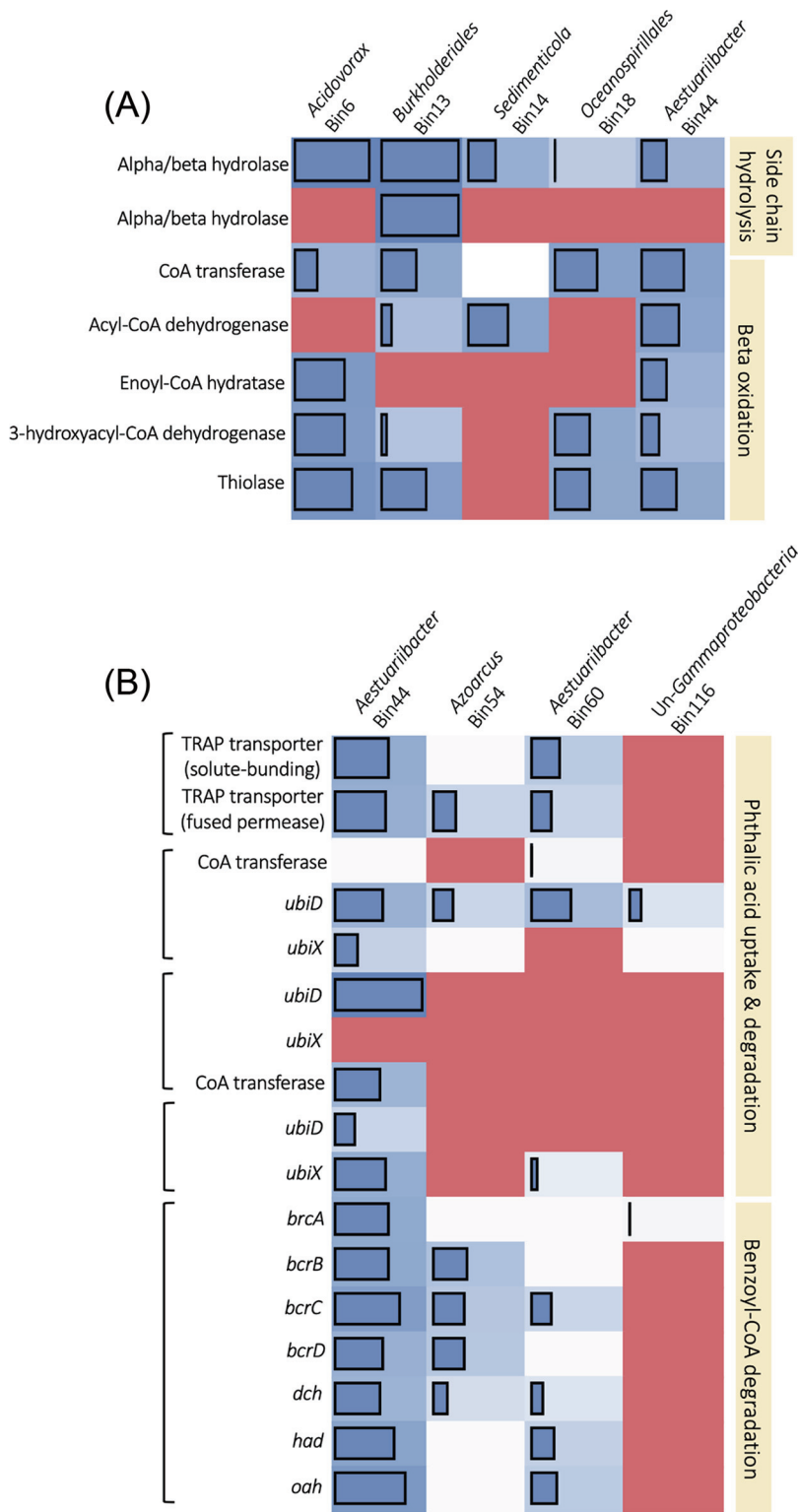


**FIG 4** Abundance of differential expression genes involved in alkyl side chain degradation (A) and *o*-phthalic acid uptake and degradation (B) in DEHP-treated sediments. Genes identified in the same contig in each binned genome were grouped in the same square brackets. Blue blocks and bars indicate the differentially expressed genes and their abundance (log CPM). White blocks denote genes that were identified but not differentially expressed. The red blocks indicate genes not recovered. The contig number, fold change, CPM, and annotation of these genes are listed in Data Set S1 in the supplemental material. *ubiD*, UbiD-like phthaloyl-CoA decarboxylase; *ubiX*, flavin prenyltransferase; *bcrABCD*, benzoyl-CoA reductase; *dch*, dienoyl-CoA hydratase; *had*, hydroxyacyl-CoA dehydrogenase; *oah*, oxoacyl-CoA hydrolase.

**TABLE 3** Differentially expressed genes related to nitrate reduction, chemotaxis, and motility in the binned genomes

Gene product (KEGG ortholog)							
Function	<i>Burkholderiales</i> Bin13	<i>Sedimenticola</i> Bin14	<i>Oceanospirillales</i> Bin18	<i>Aestuuriibacter</i> Bin44	<i>Azoarcus</i> Bin54	<i>Aestuuriibacter</i> Bin60	
Nitrate reduction	Nitrate reductase/nitrite oxidoreductase, alpha and beta subunit (K03070, K03071); nitrate reductase molybdenum cofactor assembly chaperone (K00373); nitrate reductase gamma subunit (K00374)	Nitrate/nitrite transporter (K02575, K02576); nitrate reductase/nitrite oxidoreductase, beta subunit (K03071)	Periplasmic nitrate reductase NapA (K2567)	Nitrite reductase large subunit (K00362); nitrate reductase/nitrite oxidoreductase, alpha and beta subunit (K03070, K03071); nitrate reductase catalytic subunit (K00372); nitrate reductase molybdenum cofactor assembly chaperone (K00373); nitrate reductase gamma subunit (K00374); nitrate/nitrite transporter (K02575)	Periplasmic nitrate reductase NapA (K2567); nitrate reductase/nitrite oxidoreductase, beta subunit (K03071); nitrate reductase molybdenum cofactor assembly chaperone (K00373)	Nitrate reductase/nitrite oxidoreductase, alpha and beta subunit (K03070, K03071); nitrate reductase molybdenum cofactor assembly chaperone (K00373); nitrate reductase gamma subunit (K00374); nitrate/nitrite transporter (K02575)	
Chemotaxis	Not recovered	Recovered but not differentially expressed	Chemotaxis methyltransferase CheR (K00575); chemotaxis glutaminase (K2390); methyl-accepting chemotaxis protein (K03406); chemotaxis sensor kinase CheA (K03407); chemotaxis protein CheVY (K03415; K03413); chemotaxis pili protein ChpABC (K06596, K06597, K06598)	Not recovered	Methyl-accepting chemotaxis protein (K03406); chemotaxis sensor kinase CheA (K03407); chemotaxis glutaminase (K2390); chemotaxis protein CheWY (K03408, K03413, K03415)	Chemotaxis methyltransferase CheR (K00575); chemotaxis glutaminase (K2390); chemotaxis protein MotB (K02557); methyl-accepting chemotaxis protein (K03406); chemotaxis sensor kinase CheA (K03407); purine-binding protein CheW (K3408); chemotaxis protein CheD (K3411)	
Motility	Flagellin (K02406)	Recovered but not differentially expressed	Hook-associated protein 123 (K02396, K02407, K02397); biosynthesis protein FigF (K02404); flagellin (K02406); flagellar protein FliL (K02415); biosynthesis protein FlhG (K04562)	Flagellin (K02406); hook-associated protein 2 (K02407); flagellar protein FlaG (K06603); flagellar protein FljS (K02422)	Basal-body rod protein FigBD (K02387, K02389); biosynthesis protein FigN (K02399); flagellin (K02406); hook-associated protein 2 (K02407); flagellar protein FlaG (K06603); flagellar brake protein (K21087)	Biosynthesis protein FlhAF (K02400, K02404); M-ring protein FljR (K02409); flagellum ATP synthase (K02412); hook-length control FljK (K02414); flagellar motor switch protein FljMN (K02416, K02417); biosynthesis protein FlhG (K04562)	

CheckM result revealed that the Bin60 and Bin116 genomes showed the highest (93.65%) and lowest degrees of completeness, respectively. The overall information and quality of these selected binned genomes are detailed in Table 2. We also recovered *Thauera* Bin97 and *Azoarcus* Bin394 with transport and degradation capacity for *o*-phthalic acid in the *o*-phthalic acid-treated sediments (see Table S2). The details are described in Text S1.

***Acidovorax* sp. strain 210-6 isolated from the DEHP-enriched mesocosm displayed degradation capacity for the alkyl side chains of DEHP.** To elucidate the functionality of the DEHP-enriched sediment bacteria, we cultured and isolated the DEHP degrader *Acidovorax* sp. strain 210-6 from the SDN1 mesocosm and sequenced its genome (accession number [no.] [GCA\\_010020825.1](#)). The growth curve measurement and metabolite profile analysis showed that strain 210-6 utilized DEHP, MEHP, and 2-ethyl-1-hexanol as sole carbon and energy sources in a denitrifying medium (Fig. 5). Notably, we observed the accumulation of *o*-phthalic acid in the DEHP- and MEHP-fed cultures concomitant with the consumption of these substrates (Fig. 5A). The optical density (OD) at 600 nm did not increase when either *o*-phthalic acid or benzoic acid was present as the sole carbon and energy sources, and these substrates were not apparently consumed.

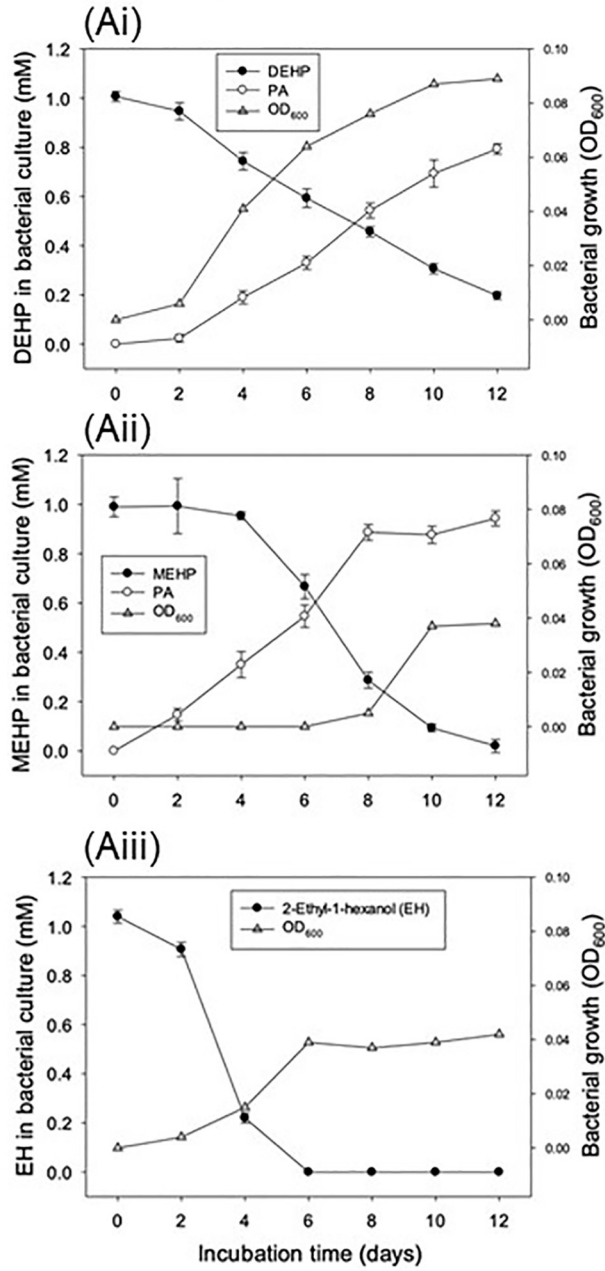
The strain 210-6 genome contained three identical copies of 16S rRNA genes, which displayed 97.7% sequence similarity to the 16S rRNA gene of *Acidovorax valerianellae* DSM 16619. The chromosome and plasmid harbor 29 genes encoding alpha/beta hydrolase. Consistent with their growth profiles, genes involved in the degradation of *o*-phthalic acid were not identified in the genome of strain 210-6. We did not observe any DEHP degradation activity when we used the soluble proteins of *Acidovorax* sp. 210-6. However, SDS-PAGE analysis of the active fraction obtained from extracellular proteins showed a protein band corresponding to an approximate molecular mass of 50 kDa (Fig. 5Bi). The purified protein transformed DEHP into *o*-phthalic acid within 12 h (Fig. 5Bii), underscoring its side chain hydrolysis activity. Moreover, the temporal accumulation of MEHP was not observed, suggesting the hydrolysis of DEHP into MEHP as the rate-limiting step. The results of liquid chromatography (LC)-tandem mass spectrometry (MS/MS) analysis revealed that one alpha/beta hydrolase, [NCU65476](#) (encoded by a chromosomal gene), displayed the highest posterior error probabilities (PEP) score for tryptic peptides originating from the active fraction. Notably, the genes for [NCU65476](#) and for its two identical copies, namely, [NCU65467](#) and [NCU65472](#), were located in the same gene cluster on the chromosome (Fig. 5C); each gene carried the predicted signal peptide and was flanked by transposase elements.

#### **Phylogenetic analysis of phthaloyl-CoA decarboxylases and DEHP/MEHP hydrolases.**

The unrooted maximum likelihood tree of phthaloyl-CoA decarboxylase showed that eight genes annotated as phthaloyl-CoA decarboxylase in the gammaproteobacterial bins (except for [k141\\_3428055\\_1](#), [k141\\_2680687\\_1](#), and [k141\\_1830739\\_7](#)) formed a distinct clade, whereas another phthaloyl-CoA decarboxylase gene ([k141\\_1104744\\_1](#)) recovered in *Azoarcus* Bin394 was placed in the same clade with phthaloyl-CoA decarboxylase genes derived from denitrifying betaproteobacteria (*A. aromaticum* DSM 19081, *A. toluclasticus* ATCC 700605, *T. chlorobenzoica* DSM 18012, and *Azoarcus* sp. PA01). These two clades were distinct from the phthaloyl-CoA decarboxylase of sulfate-reducing *Deltaproteobacteria* (*Desulfosarcina cetonica* DSM 7267, and *Desulfobaccula toluolica* DSM 7467) (Fig. 6). Other UbiD family decarboxylases, namely, 2,5-furandicarboxylate decarboxylase, 3-octaprenyl-4-hydroxybenzoate decarboxylase, phenolic acid decarboxylase subunit C, phenylphosphate carboxylase subunit alpha, and phenylphosphate carboxylase subunit beta, were placed into the same clades along with their homologs identified in DEHP-treated mesocosms (see Fig. S5). In addition, we noted that UbiD from *Acidovorax* sp. strain 210-6 (protein identifier [ID] [NCU67919](#)) was grouped into the clade with other 3-octaprenyl-4-hydroxybenzoate decarboxylase sequences in line with its inability to degrade *o*-phthalic acid.

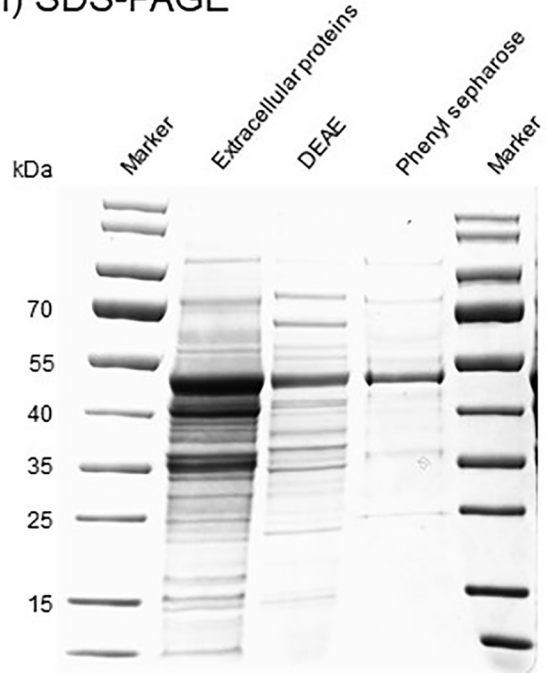
In the unrooted maximum likelihood tree of hydrolases (Fig. 7), hydrolases involved in the aerobic side chain degradation of monoalkyl PAEs (from aerobic *Rhodococcus* spp. and *Gordonia* spp.) formed a distinct lineage. Most of the hydrolases involved in the degradation

### (A) Bacterial growth

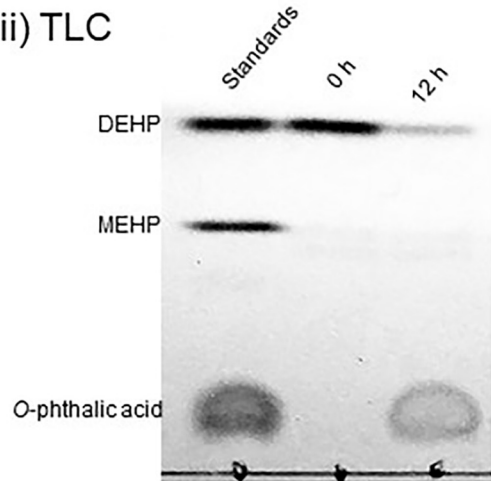


### (B) Hydrolase purification

#### (Bi) SDS-PAGE



#### (Bii) TLC



### (C) DEHP/MEHP hydrolase genes

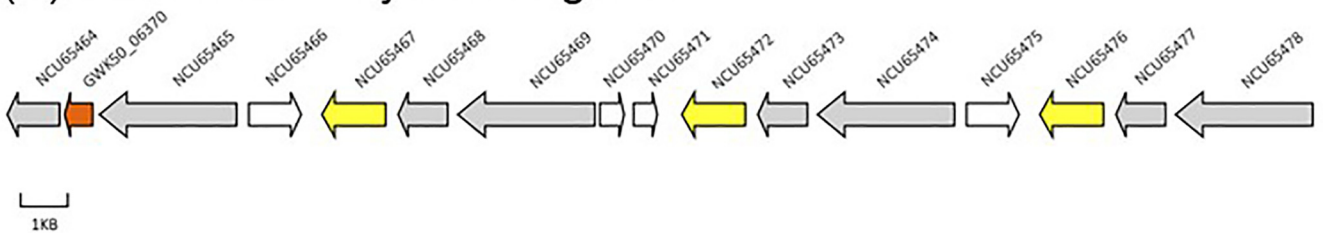


**FIG 5** Functional characterization of *Acidovorax* sp. strain 210-6 and its DEHP/MEHP hydrolase. (A) Anaerobic growth of the strain 210-6 with DEHP (Ai), MEHP (Aii), and 2-ethylhexanol (EH) (Aiii). DEHP, MEHP, and o-phthalic acid (PA) were quantified using UPLC-APCI-HRMS, whereas EH was quantified using GC-MS. (B) Purification and characterization of DEHP/MEHP hydrolase. (Bi) SDS-PAGE (4% to 12%) indicated the purification of the DEHP/MEHP hydrolase

(Continued on next page)

of dialkyl PAEs from several aerobes—*Acinetobacter* sp. M673, *Gordonia* sp. YC-JH1, *Sulfobacillus Acidophilus* DSM 1032, and *Sphingobium* sp. SM42, and PAMC26605—were also placed into the same clade, except for hydrolases involved in side chain degradation of di-*n*-butyl phthalate (from *Sphingobium* sp. SM42) and DEHP (from *Gordonia* sp. 5F). In contrast, we observed that all DEHP/MEHP hydrolases from denitrifying bacteria and bins formed a distinct clade. Moreover, four DEHP/MEHP hydrolases (NCU68007, NCU65467, NCU65472, and NCU65476) from *Acidovorax* sp. strain 210-6, three putative hydrolases (K141\_4060503\_4, K141\_3815848\_2, and K141\_2812817\_2) from betaproteobacterial bins, as well as three hypothetical proteins from the two strains of *Pigmentiphaga* and uncultured *Burkholderiales* bacterium were in the same lineage. These hypothetical proteins also belonged to the alpha/beta hydrolase family IPR029058 with predicted signal peptides (Table 1). Other putative DEHP hydrolases—K141\_138169\_2, K141\_2938615\_2, and K141\_853245\_1—derived from gammaproteobacterial bins were in different lineages.

**Transposon genes in contigs and gene clusters with key enzymes for DEHP degradation.** In *Burkholderiales* Bin13, we noted that two putative DEHP/MEHP hydrolase genes were flanked by transposon genes in two contigs (Fig. 8). Moreover, hydrolase genes in the genomes of the *Burkholderiales* bacterium RIFCSPLOWO2 and *Pigmentiphaga* sp. D-2 that displayed high AAI (99.7% and 72.2%, respectively) to the DEHP/MEHP hydrolase gene (encoding NCU65476) of *Acidovorax* sp. strain 210-6 were flanked by transposon genes (Fig. 8). A similar arrangement was observed in *Aestuarius* Bin44, in which genes involved in anaerobic *o*-phthalic acid degradation—namely, those encoding flavin prenyltransferase, phthaloyl-CoA decarboxylase, and CoA transferase—were adjunct to transposon elements (Fig. 8).

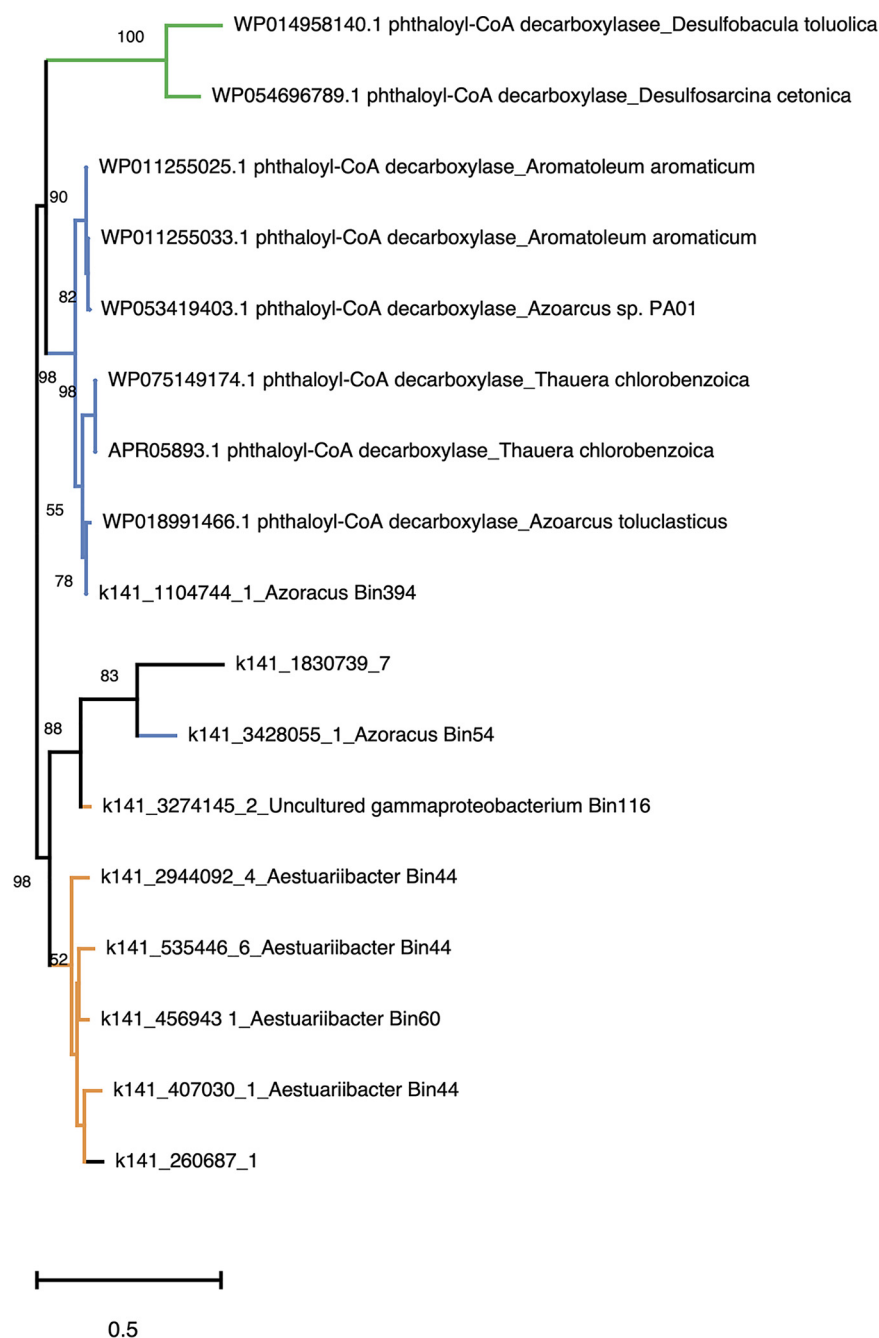
## DISCUSSION

In this study, we used an integrated multi-omics approach to identify DEHP degraders and elucidate the degradation mechanisms in urban estuarine sediments containing much accumulated DEHP. Several lines of evidence suggest that DEHP degradation in estuarine sediments mainly occurs through synergistic microbial metabolism: (i) in DEHP-treated mesocosms, various betaproteobacteria and gammaproteobacteria were enriched, and (ii) most of the binned genomes lacked the complete set of degradation genes for DEHP; instead, these bins possessed genes either for alkyl side chains or for *o*-phthalic acid degradation. A similar observation was made in sediment isolate *Acidovorax* sp. strain 210-6, which could degrade only alkyl side chains but not *o*-phthalic acid. This finding is different from those of most biodegradation studies, which have indicated that the uptake and mineralization of organic micropollutants are carried out by single bacterial isolates. For example, bacterial community structure analysis indicates that the complete mineralization of endocrine-disrupting steroids in sludge and sediment mesocosms is achieved by a single betaproteobacterial genus (24–26). Moreover, several denitrifying bacteria capable of complete steroid degradation have been isolated from steroid-treated mesocosms (27).

Synergistic networks between diverse bacteria are reportedly required for complete DEHP degradation (28–30); however, the corresponding studies have not fully elucidated the biochemical mechanisms involved in this bioprocess or provided insights into the degradation role of each microorganism. In our DEHP-treated mesocosms, six putative DEHP hydrolase genes (four with a predicted signal peptide) were differentially expressed, and one of the hydrolases, k141\_3815854\_2, was identified in Bin6, which displayed the closest AAI to *Acidovorax* sp. HMWF018. This hydrolase exhibited 100% AAI to a putative DEHP/MEHP hydrolase gene (encoding NCU68007) (see Data

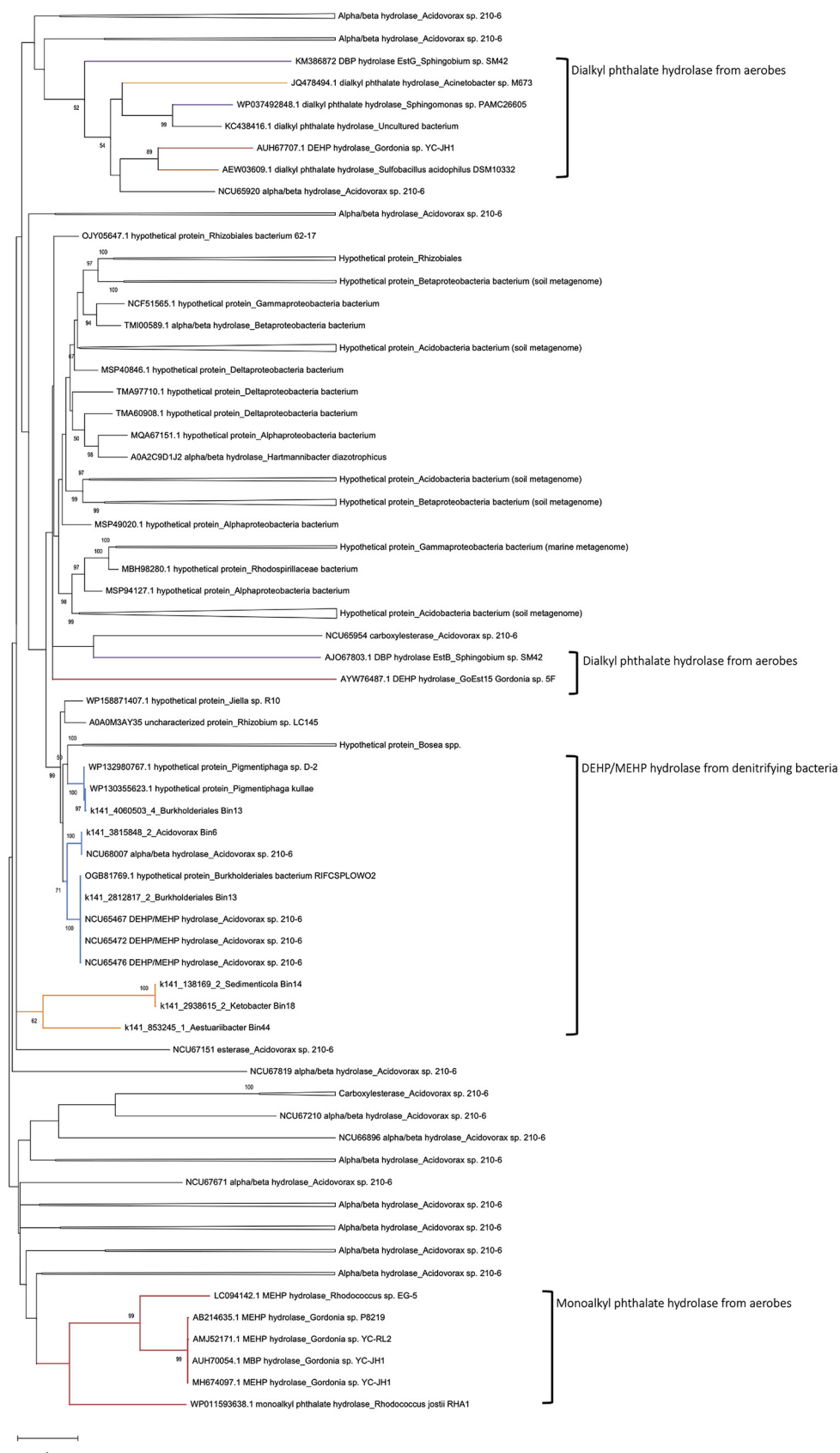
### FIG 5 Legend (Continued)

from the extracellular proteins of strain 210-6. (Bii) Thin-layer chromatography (TLC) indicated the hydrolase activity of the purified protein toward DEHP. The detected major product was PA but not MEHP. After 12 h of anaerobic incubation, metabolites were extracted with ethyl acetate, separated through TLC, and visualized by spraying the TLC plate with 30% (vol/vol) H<sub>2</sub>SO<sub>4</sub>. (C) Presence of three identical copies of hydrolase genes (NCU65467, NCU65472, and NCU65476) in the chromosome of strain 210-6. Protein ID (NCU\_) or locus tag (GW50\_) are shown for each gene. Yellow, DEHP/MEHP hydrolase; gray, transposase/integrase; white, hypothetical proteins; red, proteins not related to DEHP degradation; GWK50\_06370, FAD-dependent oxidoreductase.



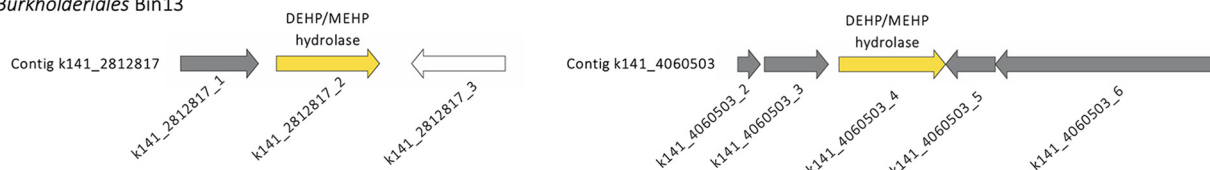
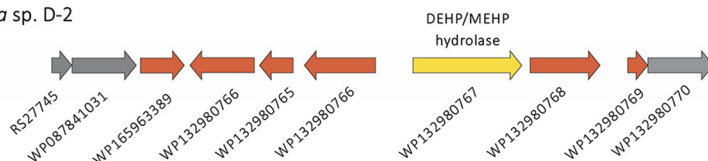
**FIG 6** Maximum likelihood tree of phthaloyl-CoA decarboxylase from bacterial isolates and in DEHP-treated sediments. Orange branch, gammaproteobacterial nitrate-reducing phthalic acid degraders; blue branch, betaproteobacterial nitrate-reducing *o*-phthalic acid degraders; green branch, deltaproteobacterial sulfate-reducing phthalic acid degraders. Branch support of higher than 50% of the bootstrapping time is shown.

Set S1 in the supplemental material) on the plasmid of strain 210-6, suggesting that *Acidovorax* Bin6 is a DEHP side chain degrader. Furthermore, the isolation and characterization of strain 210-6 confirmed *Acidovorax* spp. as active DEHP degraders in the estuarine sediments. Putative DEHP-degrading hydrolase (k141\_138169\_2) and  $\beta$ -oxidation genes for anaerobic 2-ethylhexanol degradation were identified in Bin14, and its closest taxonomy affiliation was *Sedimenticola selenatireducens*. The degradation of DEHP and other PAEs was not previously reported for the genus *Sedimenticola* (31–34). Their apparent enrichment in DEHP-treated sediments suggests that *Sedimenticola*

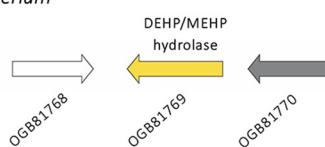
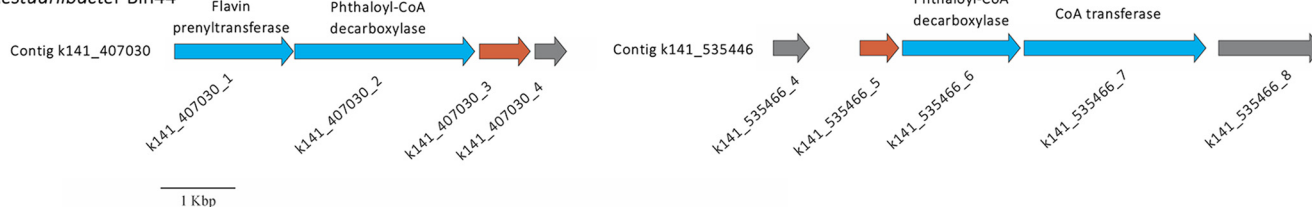


**FIG 7** Maximum likelihood tree of hydrolases involved in degradation of alkyl side chains on DEHP and other PAEs and other hydrolases from *Acidovorax* sp. strain 210-6. The phylogeny of the protein sequences from NCBI (Continued on next page)



*Burkholderiales* Bin13*Pigmentiphaga* sp. D-2*Burkholderiales bacterium*

## RIFCSPLOWO2

*Aestuuriibacter* Bin44

**FIG 8** Transposase genes in contigs or gene clusters carrying essential components for side chain hydrolysis of DEHP and *o*-phthalic acid degradation. Gray, transposase/integrase; yellow, DEHP/MEHP hydrolase; blue, genes for *o*-phthalic acid degradation; white, hypothetical proteins; red, proteins not related to DEHP degradation. Sequence references of genomes of *Pigmentiphaga* sp. D-2 and *Burkholderiales bacterium* RIFCSPLOWO2 are indicated. Full annotation of Bin13 and Bin44 is listed Data Set S1.

plays a role in DEHP degradation. The key genes involved in anaerobic *o*-phthalic acid degradation were not recovered in *Sedimenticola* Bin14; thus, we speculated that *Sedimenticola* may be involved in the alkyl side chain degradation of DEHP in denitrifying sediments. The slow transformation of DEHP into MEHP and the accumulation of trace amounts of downstream metabolites (MEHP and *o*-phthalic acid) in both DEHP-treated mesocosms and *Acidovorax* sp. culture suggested DEHP hydrolysis as a bottleneck in the anaerobic DEHP degradation pathway. Future studies may focus on improving activities of the extracellular DEHP hydrolases. For example, the enhancement of DEHP solubility likely could improve the DEHP biodegradation, since DEHP solubility is below 3 mg/liter (13). Moreover, the optimization of pH and temperature and required cofactors for the DEHP/MEHP hydrolase remain to be characterized. Site-directed mutagenesis, on the other hand, could be employed to evolve the DEHP hydrolases into more competent biocatalysts.

On the basis of the profiles of DEHP-derived metabolites and changes in community structures, as well as the taxonomy and functionality of binned genomes, we propose that in the examined denitrifying sediments, complete DEHP degradation requires synergistic metabolism. *Acidovorax* (Bin6), unclassified betaproteobacterium *Burkholderiaceae*

**FIG 7** Legend (Continued)

and UniProt with an identity  $\geq 40\%$  similar to [NCU65467](#) of *Acidovorax* sp. strain 210-6 was also inferred. Purple branch, aerobic alphaproteobacterial degraders; blue branch, anaerobic betaproteobacterial degraders; red branch, aerobic actinobacterial degraders; orange branch, anaerobic gammaproteobacterial degraders; brown branch, aerobic *Firmicutes* degraders. Branch support of more than 50% of the bootstrapping time is shown.

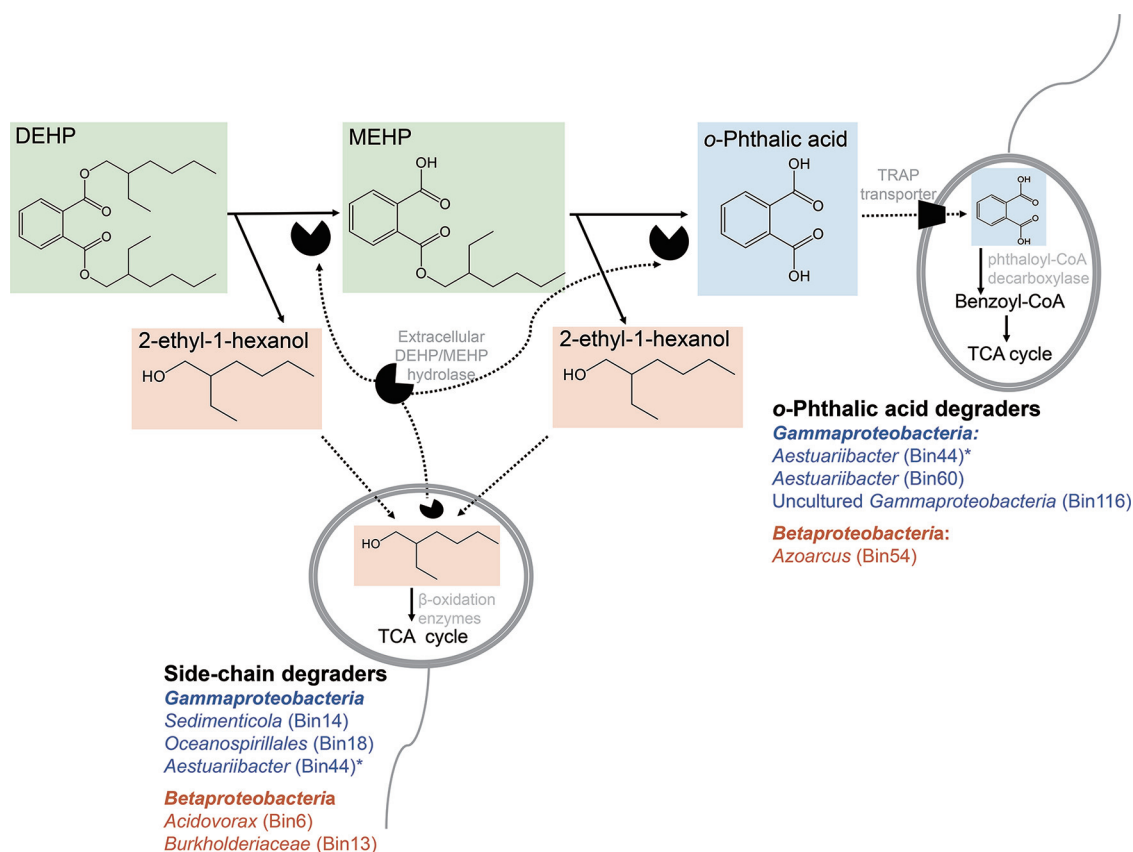


**FIG 9** Diagram of proposed DEHP degradation through microbial synergistic metabolism in denitrifying sediments. The betaproteobacterium *Acidovorax* and gammaproteobacterium *Sedimenticola* are major degraders of DEHP side chains. The resulting *o*-phthalic acid is then imported through a specific TRAP transporter and degraded by other betaproteobacteria (e.g., *Azoarcus*) and gammaproteobacteria (e.g., *Aestuariibacter*). \*, Gammaproteobacterial Bin44 has degradation capacity for both side chains and *o*-phthalic acid. Orange, *Gammaproteobacteria*; blue, *Betaproteobacteria*.

(Bin13), *Sedimenticola* (Bin14), and *Oceanospirillales* member SS1\_B\_06\_26 (Bin18) are major degraders of the alkyl side chains (namely, the 2-ethylhexanol moiety) of DEHP. The remaining *o*-phthalic acid is likely transported into bacterial cells by a specific TRAP transporter and primarily degraded by uncultured gammaproteobacterial MBE14 (Bin116) and *Aestuariibacter* (Bin60) through the anaerobic benzoyl-CoA pathway (Fig. 9). Synergistic interactions in a bisphenol A-degrading microbial community were also identified in a recent study (35), suggesting the crucial role of synergistic microbial metabolism in removing endocrine-disrupting aromatics from contaminated environments.

Our community and metagenomic analyses suggest that *Thauera* and *Azoarcus* are ecologically relevant degraders for *o*-phthalic acid. Unexpectedly, our phylogenetic and metagenomic analyses indicated that *o*-phthalic acid degraders in DEHP-treated sediments are mainly denitrifying gammaproteobacteria, revealing that the degraders for anaerobic *o*-phthalic acid are not only restricted to denitrifying betaproteobacteria (17–20) and sulfate-reducing deltaproteobacteria (*Desulfosarcina cetonica* DSM 7267 and *Desulfobacula toluolica* Tol2 [DSM 7467]) that were previously characterized (36). Moreover, whether DEHP is toxic to *Thauera* and *Azoarcus* remains unclear. An apparent decrease in the abundance of other bacteria (e.g., *Clostridiales*) can be observed due to their sensitivity to DEHP (37–39). In addition, differentially expressed genes related to chemotaxis and flagellar synthesis in DEHP-degrading *Sedimenticola* (Bin14) and *Aestuariibacter* (Bin44) as well as *o*-phthalic acid-degrading *Aestuariibacter* (Bin60) suggest that DEHP can be an attractant for not only DEHP degraders but also some *o*-phthalic acid-degrading anaerobes. Some bacteria display chemotaxis toward

substrates that they are not able to degrade (40, 41). Accordingly, we assumed that DEHP induced chemosensory responses in some *o*-phthalic acid-degrading gammaproteobacteria, enhancing their better attraction to *o*-phthalic acid produced from DEHP.

Chemotaxis has been proposed to facilitate horizontal gene transfer because the ability of bacteria to accumulate around pollutant substrates increases the possibility of the transfer of relevant catabolic genes (42). Transposon elements have been identified in the gene clusters involved in DEHP side chain hydrolysis in the genome of *Acidovorax* sp. strain 210-6 as well as in *o*-phthalic acid degradation in *A. aromaticum* DSM 19081 (on plasmid), *Azoarcus* sp. PA01 (on chromosome), and *T. chlorobenzoate* DSM 18012 (on chromosome) (19). Furthermore, Sanz et al. (43) suggested that the complete *o*-phthalic acid degradation pathway in denitrifying bacteria, together with the *o*-phthalic acid transporter gene, is successfully transferred to heterologous bacteria that are unable to use *o*-phthalic acid as a substrate. In the present study, a similar observation was made in DEHP side chain-degrading *Burkholderiales* Bin13 and *o*-phthalic acid-degrading *Aestuariibacter* Bin44. Surprisingly, the gene cluster or contig with potential DEHP-degrading hydrolases from *Pigmentiphaga* sp. D-2 and uncultured *Burkholderiales* bacterium also contained a transposase gene. These findings indicate that in the natural environment, DEHP degradation capacity may be widespread among proteobacteria due to transposon-mediated horizontal gene transfer (44); this further supports the notion that anthropogenic inputs may not only result in changes in community structures but also in ecosystem functioning (45, 46).

**Future perspective.** The estuarine and marine ecosystems have been impacted severely by plastic pollution (1). A recent study reported that several gammaproteobacterial isolates (genera *Idiomarina* and *Halomonas*) and two actinobacterial species isolates from marine plastic debris displayed DEHP degradation capacity under aerobic conditions (47), whereas degraders isolated from terrestrial ecosystems were mostly actinobacteria (genus *Rhodococcus*, *Gordonia*, and *Mycobacterium*). The interrogation of DEHP degraders, from either anaerobic or aerobic environments, may not be comprehensive to date, but this raises interesting speculation whether the taxonomy of DEHP degraders is ecosystem specific. On the other hand, the discovery of synergistic microbial networks in removing DEHP in this study suggested that the bioremediation for DEHP-contaminated ecosystems may not rely only on single bacterium, although the efficient removal of DEHP via *Rhodococcus* strains in vegetation soils has been demonstrated (48). This is congruent with a new insight that using microbial consortia with diverse degradation genes will be critical to achieve the complete mineralization of PAE-like pollutants in the future (49).

## MATERIALS AND METHODS

**Sample site and sediment collection.** In the northern part of Taiwan, up to 6 million people reside in the city of Taipei located in the basin of the Tamsui River and Keelung River. Our sampling site, Guandu estuary (25°6'59.56"N, 121°27'46.99"E) is located downstream of these two rivers and receives sewage discharges and waste effluent from the Taipei metropolitan area. The profile of PAEs in river ecosystems in Taiwan has been identified; the average DEHP concentration in Tamsui River sediments was 2.3  $\mu\text{g/g}$ ; other PAEs, namely, diethyl phthalate (DEP), dipropyl phthalate (DPP), di-*n*-butyl phthalate (DBP), diphenyl phthalate (DPhP), benzylbutyl phthalate (BBP), dihexyl phthalate (DHP), and dicyclohexyl phthalate (DCP), were either not detected or were detected in concentrations lower than 0.5  $\mu\text{g/g}$  (50). Nitrate and denitrifying bacteria were abundant in the subsurface sediments (5 to 10 cm) of Guandu estuary (51). During the low tide that occurred on 2 July 2018, two independent subsurface sediment and river water samples were collected as described previously (25). These samples were stored at 4°C and transported to the laboratory within 1 h for mesocosm incubation of denitrifying sediments.

**Mesocosm incubation of denitrifying sediments with DEHP, benzoic acid, or *o*-phthalic acid.** Mesocosm experiments were performed in 1-liter sterilized serum bottles containing subsurface sediments (approximately 200 g) and river water (approximately 800 ml). Four types of mesocosm (two replicates in each)—10 mM sodium nitrate and 1 mM DEHP (SDN mesocosm), 10 mM sodium nitrate and 1 mM *o*-phthalic acid (SPN mesocosm), 10 mM sodium nitrate and 1 mM benzoic acid (SBN mesocosms), and 10 mM nitrate only (SN mesocosm as the control)—were prepared under anoxic conditions by purging 80% (vol/vol) of nitrogen gas and 20% (vol/vol) of carbon dioxide into serum bottles sealed with butyl rubber stoppers. All mesocosms were further reduced with 0.5 mM  $\text{Na}_2\text{S}$  to neutralize oxygen and incubated at 25°C with agitation. The consumption of nitrate was monitored using the Spectroquant

nitrate test kit HC707906 (Merck, Germany). Sodium nitrate (10 mM) was resupplied when nitrate was depleted until the exogenous substrates were completely degraded. Samples of river water and sediment mixture (approximately 10 ml) were obtained from each mesocosm every 2 or 3 days, stored at  $-80^{\circ}\text{C}$  for metabolite extraction, and preserved in LifeGuard soil preservation solution (Qiagen, Germany) for total DNA/RNA extraction. All chemicals were purchased from Sigma-Aldrich, Merck KGaA (St. Louis, MO, USA).

**UPLC-APCI-HRMS analysis of DEHP-derived metabolites.** Hydrophobic non-CoA thioester metabolites in the mesocosms (SDN, SPN, and SBN samples) were extracted using ethyl acetate as described previously (25). Crude extracts were then applied in UPLC-MS with UPLC coupled to an APCI-mass spectrometer to identify and quantify metabolites. DEHP and its metabolites were first separated using a reversed-phase  $\text{C}_{18}$  column (Acquity UPLC BEH  $\text{C}_{18}$ ,  $1.7\ \mu\text{m}$ , 100 by 2.1 mm; Waters) at a flow rate of 0.3 ml/min at  $65^{\circ}\text{C}$  (oven temperature). The mobile phase was a mixture of two solutions: solution A (0.1% formic acid [vol/vol] in 2% acetonitrile) and solution B (0.1% formic acid [vol/vol] in isopropanol). Separation was achieved using a gradient of solvent B from 1% to 99% over 7 min. APCI-MS analysis was performed using an Orbitrap Elite hybrid ion trap-Orbitrap mass spectrometer (Thermo Fisher Scientific, Waltham, MA, USA) equipped with a standard APCI source. MS data were collected in the positive ionization mode (parent scan range, 100 to 500  $m/z$ ). The capillary and APCI vaporizer temperatures were  $120^{\circ}\text{C}$  and  $400^{\circ}\text{C}$ , respectively; the sheath, auxiliary, and sweep gas flow rates were 40, 5, and 2 arbitrary units, respectively. The source voltage was 6 kV, and the current was  $15\ \mu\text{A}$ . The elemental composition of individual adduct ions was predicted using Xcalibur software V2.2 (Thermo Fisher Scientific). The following authentic standards were purchased from Sigma-Aldrich: DEHP, MEHP, *o*-phthalic acid, and benzoic acid.

**Gas chromatography-MS analysis of 2-ethyl-1-hexanol.** Quantification of the remaining 2-ethyl-1-hexanol in bacterial cultures was performed through GC on an HP 5890 series II GC device coupled to a 5972 series mass-selective detector (Hewlett-Packard, Palo Alto, CA, USA). A fused-silica capillary GC column (DB-1ms, 60 m, 0.25-mm inside diameter [i.d.]; Agilent J & W Scientific, Folsom, USA) chemically bonded with a 100% dimethylpolysiloxane stationary phase (0.25-mm film thickness) was used. The sample was inserted in the splitless mode by using helium as a carrier gas. Initially, the oven temperature was maintained at  $60^{\circ}\text{C}$  and then increased to  $95^{\circ}\text{C}$  at the rate of  $2^{\circ}\text{C}/\text{min}$ . Once the temperature had been maintained at  $95^{\circ}\text{C}$  for 1 min, it was increased to  $120^{\circ}\text{C}$  at a rate of  $3^{\circ}\text{C}/\text{min}$  and then maintained at  $120^{\circ}\text{C}$  for 2 min. Subsequently, the temperature was further increased to  $180^{\circ}\text{C}$  at the rate of  $6^{\circ}\text{C}/\text{min}$  and maintained at  $180^{\circ}\text{C}$  for 2 min. Electron impact ionization was used as an ionization source for the GC-MS analysis at 70 eV. Data acquisition was performed in full-scan mode from 50 to 300  $m/z$  over a scan duration of 0.5 s. *n*-Hexane (as a blank) was run between samples to remove contamination. Mass calibration was performed using perfluorotributylamine. Authentic standard 2-ethyl-1-hexanol was purchased from Sigma-Aldrich.

**DNA extraction and 16S rRNA gene amplicon sequencing.** The bacterial community structure of each mesocosm and temporal changes (day 0 to day 25 for the SN, SBN, and SPN mesocosms and day 0 to day 30 for the SDN mesocosm; two replicates for each) were identified using an Illumina MiSeq platform. DNA was extracted from treated sediments by using the PowerSoil DNA isolation kit (Qiagen, Germany). The 16S amplicon libraries targeting the V3-V4 regions of 16S rRNA genes (52) were prepared according to the Illumina 16S metagenomic sequencing library preparation guide by using a gel purification approach as described previously (24). In total, 96 libraries were generated, and their profiles were analyzed using the Bioanalyzer 2100 with a high-sensitivity DNA kit (Agilent, USA). To ensure the evenness of library pooling, all libraries were subjected to quantitative PCR (qPCR) for normalization by using a Kapa library quantification kit to obtain molar concentrations. For sequencing, the pooled library was run on an Illumina MiSeq sequencer with MiSeq reagent kit V3 (paired end; 2 by 300 bp).

**Bioinformatics processing and taxonomic assignment for 16S amplicon sequencing.** MiSeq sequencing generated 27,848,006 reads from 96 sediment samples. USEARCH v11 (53) was used for paired-reads assembly, quality filtering, length trimming, and UPARSE OTU clustering (54). The representative sequences of OTUs were taxonomically assigned against Silva release 132 (55) by using mothur v1.41.3 (56). Silva release 132 reclassifies *Betaproteobacteria* as an order of *Gammaproteobacteria*. For readability, the abundances of *Gammaproteobacteria* and *Betaproteobacteria* were calculated separately. Less abundant OTUs from all samples (count of  $<2$  per OTU with a prevalence of  $<20\%$  in 96 samples) were removed and then normalized through cumulative sum scaling (57) by using MicrobiomeAnalyst (58). Similarities between microbial communities among differently treated sediments (SN, SBN, SPN, and SDN) were determined by performing principal-coordinate analysis (PCoA) in MicrobiomeAnalyst on the basis of the weighted UniFrac distance matrix (genus level). The UniFrac distance was calculated according to the neighbor-joining phylogenetic tree file generated by the MUSCLE algorithm (59). To determine the degraders for benzoic acid, *o*-phthalic acid, and DEHP, we first selected a large increase in relative abundance at the bacterial class level. We applied the analysis of variance (ANOVA) test in MetaboAnalyst 4.0 (60) to identify the bacterial genera in selected classes exhibiting the highest differences in abundance among different mesocosms.

**Metagenomic and metatranscriptomic sequencing.** To identify genes responding to exogenous DEHP and *o*-phthalic acid in denitrifying sediments, the total DNA and RNA of SDN1\_day14, SDN2\_day14, SPN1\_day7, and SPN2\_day7 were used for metagenome and metatranscriptome analyses. Total DNA and RNA were extracted using the PowerSoil DNA isolation kit and RNeasy PowerSoil total RNA kit (Qiagen, Germany), respectively. For shotgun metagenomic sequencing, the quality of DNA was examined using Fragment Analyzer (Agilent, USA), and Kapa HyperPrep kits (Kapa Biosystems, USA) were used for constructing four DNA libraries. The prepared libraries with average fragment sizes from

451 to 461 bp were sequenced using an Illumina HiSeq 2500 sequencer with a HiSeq TruSeq Rapid Duo cBot sample loading kit and HiSeq Rapid PE cluster kit v2 (paired-end), yielding 108,689,404 reads for SDN1\_day16, 96,381,152 reads for SDN2\_day16, 92,719,398 reads for SPN1\_day7, and 94,391,656 reads for SPN2\_day7.

For metatranscriptomic sequencing, the quality of RNA (RNA integrity number from 7.5 to 9.4) was examined using the Bioanalyzer 2100 system with an RNA 6000 Nano kit (Agilent, USA) before using the Ribo-Zero rRNA removal kit (Illumina) and TruSeq Stranded LT mRNA library prep kit v2 as described previously (24). The four prepared libraries with average fragment sizes from 328 to 351 bp were sequenced using an Illumina HiSeq 2500 sequencer, yielding 97,486,966 reads for SDN1\_day14, 92,150,650 reads for SDN2\_day14, 94,830,584 reads for SPN1\_day7, and 93,982,586 reads for SPN2\_day7.

**Quality trimming, assembly, gene prediction, and binning of the metagenome.** Raw reads with low quality (quality score of  $<30$ ) and short length (length of  $<36$  bp) from four metagenomes—SDN1\_day14, SDN2\_day14, SPN1\_day7, and SPN2\_day7—were trimmed using Trimmomatic v0.39 (61). The trimmed reads from all metagenomes were assembled into a single assembly by using Megahit v1.1.4 with the default setting (62). Protein-coding genes were predicted using Prodigal 2.6.3 in the metagenome mode (63). To recover genomes from the metagenome assembly, a binning algorithm, MaxBin 2.2.7, was applied (64). The taxonomy affiliation of binned genomes was determined using the following steps. First, the amino acid sequences of predicted protein-coding genes were mapped against the NCBI nonredundant protein database by using DIAMOND v0.9.26 (65) with a cutoff E value of  $1 \times e^{-5}$ . Second, the closest taxonomic hit and the AAI of each predicted gene were extracted. Finally, the closest species were selected on the basis of the majority of hits, and AAIs were averaged to be the AAI between the binned genome and its closest species. CheckM v1.07 (66) was used to examine the completeness and contamination of binned genomes. Other information regarding binned genomes was assessed using QUAST 5.0.2 (67).

**Gene quantification and differential gene expression analysis.** After performing quality trimming by using Trimmomatic v0.39 (61), we mapped metatranscriptomic reads to the metagenome assembly by using Bowtie 2 2.3.5.1 (68) and quantified them using featureCounts (under Subreads release 1.6.4.). The read count table from featureCounts was applied to edgeR 3.26.7 (69) to analyze DGE between SDN and SPN communities with two biological replicates. Genes with a  $\log_2$  fold change ( $\log_2$  FC) value of  $\geq 2$ , a false discovery rate (FDR) of  $\leq 0.05$ , and an adjusted  $P$  value of  $< 0.05$  were designated differentially expressed genes. The quantity of differentially expressed genes is presented as the count per million (CPM).

**Search for genes encoding MEHP transporter, DEHP/MEHP hydrolase, *o*-phthalic acid transporter, and phthaloyl-CoA decarboxylase.** The hidden Markov model (HMM) was employed to identify the DEHP transporter and DEHP hydrolase involved in alkyl side chain degradation of DEHP. The protein sequences of the DEHP hydrolase (NCU65476) of *Acidovorax* sp. strain 210-6 and MEHP transporter (WP\_007297306.1) identified in *Rhodococcus jostii* RHA1 (70) were used for generating two HMM profiles. The TRAP transporter and UbiD-like phthaloyl-CoA decarboxylase involved in *o*-phthalic acid uptake and degradation were also searched using the HMM (<http://hmmer.org>; v3.2.1) based on the six amino acid sequences of phthaloyl-CoA decarboxylase determined from nitrate-reducing and sulfate-reducing *o*-phthalic acid degraders (19, 36). These HMMs were then used to search against the amino acid sequences of differentially expressed genes from SDN communities. InterPro (71) and SignalP 5.0 (72) web-servers were applied to predict protein family and the signal peptide of selective hydrolases, respectively.

**General gene annotation.** The amino acid sequences of differentially expressed genes from SDN communities were annotated against the RefSeq nonredundant protein database (release 94) (73) using DIAMOND v0.9.26 with a cutoff E value of  $1 \times e^{-5}$  (65) and the ortholog-based eggNOG mapper 5.0 (74). The HMMER-based KofamKOALA (75) was employed to annotate binned genomes containing genes encoding DEHP hydrolase and phthaloyl-CoA decarboxylase that were identified in this study.  $\beta$ -Oxidation genes, namely, those encoding CoA transferase, acyl-CoA dehydrogenase, enoyl-CoA hydratase, and 3-hydroxyacyl-CoA dehydrogenase and thiolase, were selected if these genes were not an adjunct to any genes involved in aromatics degradation or amino acid metabolism. In addition, we used blastp in the NCBI or UniProt database to annotate gene function manually.

**Isolation of DEHP-degrading *Acidovorax* sp. strain 210-6.** On day 16, the DEHP-treated estuarine mesocosm (~20 ml) was transferred into a 250-ml serum bottle containing defined mineral minimal medium (200 ml) with DEHP (1 mM) as the sole carbon source and electron donor as well as sodium nitrate (10 mM) as the electron acceptor. The defined medium was prepared according to an established protocol described previously (25). After the degradation of almost all DEHP added to the medium, the culture was serially diluted ( $10^{-1}$  to  $10^{-7}$ ) and transferred to other serum bottles with the same defined medium for further cultivation. The fourth subculture containing highly enriched DEHP-degrading denitrifier was spread on tryptone soy agar containing DEHP (1 mM) to obtain a single colony. Most colonies were identified as *Acidovorax* spp. in the DEHP-containing plates through PCR by using the universal primers of the bacterial 16S rRNA gene (27F and 1492R) (52). *Acidovorax* colonies were cultivated in the aforementioned defined medium to confirm their function. The isolate cultures were used to test their utilization of other DEHP-related substrates, including MEHP, 2-ethyl-1-hexanol, *o*-phthalic acid, and benzoic acid.

**Genome sequencing, assembly, and annotation for *Acidovorax* sp. strain 210-6.** The genomic DNA of *Acidovorax* sp. 210-6 was extracted using a Prest Mini genomic DNA (gDNA) bacteria kit (Geneaid, Taiwan). The integrity of DNA was examined using Fragment Analyzer (Agilent, USA), showing the major peak size at 35 kb. The PacBio shotgun library was constructed according to the manufacturer's multiplexed bacterial protocol for the SMRTbell Express TPK 2.0 kit (PacBio). Briefly, gDNA was

sheared using Megaruptor 2 (Diagenode) to an average size of 8.9 kb, purified, and condensed using AMPure. Single-stranded DNA was removed using nucleases provided in the kit. Fragments were then subjected to end repair, A tailing, and ligation to the adaptor of barcoded overhang adapter kit 8A. A DNA size of 6 to 20 kb was selected using the BluePippin gel cassette (Sage). The final library showed an average size of 8.5 kb.

PacBio sequencing was carried out using the Sequel sequencing kit 3.0 with SMRT Cell 1M v3 LR and run on a Sequel sequencer, and the read file was generated from SMRTlink ICS v6.0. The *de novo* assembly was conducted using HGAP4.0 on SMRTlink v8.0 with a coverage depth of 258 $\times$ , resulting in three polished contigs. The NCBI Prokaryotic Genome Annotation Pipeline was applied for genome annotation. The gene clusters encoding [NCU65476](#) were visualized using Gene Graphics.

**Purification of extracellular DEHP/MEHP hydrolase from strain 210-6.** The *Acidovorax* sp. 210-6 culture (2 liters) grown on DEHP was centrifuged at 10,000  $\times g$  for 15 min to pellet down the bacterial cells, cell debris, and residual DEHP. Extracellular proteins (10  $\mu\text{g}/\text{ml}$ ; totally, 700 ml) were filtered through a 0.22- $\mu\text{m}$  nitrocellulose membrane (47-mm diameter; Millipore) and concentrated using the Amicon Ultra centrifugal filters to 7 ml (cutoff, 30 kDa). The resulting proteins were purified using the AKTA start purification system through DEAE Sepharose Fast Flow packed in the XK16 column (GE Healthcare, USA), followed by another purification using phenyl Sepharose (GE Healthcare, USA).

**Proteomic analysis.** For protein identification, active protein fractions were further separated by sodium dodecyl sulfate-polyacrylamide gel electrophoresis (SDS-PAGE) (4% to 20% bis-Tris Gel; GenScript, USA). Proteins in the gel slices were eluted in HEPES- $\text{K}^+$  buffer (50 mM, pH 8.0) and trypsin digested. The proteomic analysis was performed using an LC-nESI-Q Exactive MS model (Thermo Fisher Scientific, USA) coupled with an on-line nanoUHPLC (Dionex UltiMate 3000 Binary RSLCnano). Protein identification was performed using Proteome Discoverer software (v1.4; Thermo Fisher Scientific) with the SEQUEST search engine against all the protein sequences of the genome and the plasmids of *Acidovorax* sp. strain 210-6. All peptides were filtered with a *q* value threshold of 0.01 (false discovery rate of 1%), and proteins were filtered with a minimum of two peptides per protein, wherein only rank 1 peptides and the peptides in top-scored proteins were counted.

**DEHP and MEHP hydrolase activity assay.** We used the estuarine water to culture the sediment mesocosms, which has a pH at approximately 8.0. Thus, the hydrolase activities of protein fractions were determined in 50 mM HEPES- $\text{K}^+$  buffer (pH 8.0) containing 0.2 mM DEHP or MEHP. The reaction was carried out at 30°C and sampled at 0 and 12 h. The remaining DEHP, MEHP, or *o*-phthalic acid in each reaction was extracted by ethyl acetate and detected using thin-layer chromatography and UPLC-APCI-HRMS.

**Phylogenetic analyses for phthaloyl-CoA decarboxylase and DEHP/MEHP hydrolase.** Maximum likelihood trees were constructed in MEGA X (76) to elucidate the phylogeny of UbiD family decarboxylase and alpha/beta hydrolase. All amino acid sequences for this analysis were aligned without truncation by using MUSCLE (59) in MEGA X. The best amino acid substitution model for each tree was determined using the Model Test in MEGA X. The branch support was determined by bootstrapping 1,000 times.

For the UbiD tree, apart from the amino acid sequences of *ubiD* in the *Acidovorax* sp. strain 210-6 genome and DGE in SDN metagenome, we selected 100 amino acid sequences of 3-octaprenyl-4-hydroxybenzoate carboxylase and four phenolic acid decarboxylase sequences (all manually annotated and reviewed) from the UniProt database as references. One sequence of phthaloyl-CoA decarboxylase from *Azoarcus* Bin394 and eight sequences of phthaloyl-CoA decarboxylase from anaerobic phthalate degraders (19, 36), one sequence of iso-phthaloyl-CoA decarboxylase and its closely related sequences (phenolic acid decarboxylase subunit C) (77), and one sequence each of 2,5-furandicarboxylate decarboxylase, phenolic acid decarboxylase subunit C, and phenylphosphate carboxylase subunit alpha and beta were also included for this phylogenetic analysis. The UbiD maximum likelihood tree was constructed using the LG substitution model plus the gamma distribution rate.

The phylogeny of hydrolases responsible for the alkyl side chain degradation on PAEs was also constructed. The amino acid sequences of alpha/beta hydrolases in the genome of *Acidovorax* sp. 210-6 and hydrolases derived from several aerobic *o*-phthalic acid-degrading *Actinobacteria* (14–16, 70, 78–80), *Alphaproteobacteria* (81, 82), *Firmicutes* (83), *Gammaproteobacteria* (84), and uncultured bacterium (85) were used for inferring the maximum likelihood tree. The bacterial source, substrate specificity, and accession numbers of these aerobic hydrolases are listed in Table S1 in the supplemental material. We included the amino acid sequences of the most similar proteins to [NCU65476](#) (identity  $\geq 40\%$ ) from the NCBI and UniProt databases. The maximum likelihood tree was constructed under the WAG+F substitution model plus the gamma distribution rate.

**Data availability.** The raw reads of 16S amplicon sequencing from SN, SBN, SDN, and SPN communities were deposited in Sequence Read Archive (SRA) of NCBI under accession [PRJNA604667](#). The raw reads of the metagenome and metatranscriptome of SDN\_day14 and SPN\_day7 are available under the SRA experiments of [PRJNA602375](#) in NCBI. The strain 210-6 genome was deposited in NCBI under accession [GCA\\_010020825.1](#).

## SUPPLEMENTAL MATERIAL

Supplemental material is available online only.

**DATA SET S1**, XLSX file, 0.1 MB.

**TEXT S1**, PDF file, 0.1 MB.

**FIG S1**, JPG file, 1.2 MB.

**FIG S2**, JPG file, 0.9 MB.

**FIG S3**, JPG file, 0.8 MB.

**FIG S4**, JPG file, 1.2 MB.

**FIG S5**, JPG file, 1.4 MB.

**TABLE S1**, PDF file, 0.1 MB.

**TABLE S2**, PDF file, 0.01 MB.

## ACKNOWLEDGMENTS

This study was supported by the Ministry of Science and Technology of Taiwan (MOST 109-2221-E-001-002 and 110-2222-E-008-002) and Academia Sinica Career Development Award (AS-CDA-110-L13). Yi-Lung Chen is supported by Research Grants for New Teachers of College of Science, Soochow University, Taiwan. Po-Hsiang Wang is supported by the Research and Development Office and Research Center for Sustainable Environmental Technology, National Central University, Taiwan.

We thank the High Throughput Genomics Core Facility hosted by the Biodiversity Research Center at Academia Sinica for conducting the next-generation sequencing experiments. This core facility is funded by the Academia Sinica Core Facility and Innovative Instrument Project (AS-CFII-108-114). We also thank Yu-Ching Wu for performing UPLC-HRMS at the Small Molecule Metabolomics Core Facility, Institute of Plant and Microbial Biology.

We have no conflicts of interest to declare.

## REFERENCES

- Geyer R, Jambeck JR, Law KL. 2017. Production, use, and fate of all plastics ever made. *Sci Adv* 3:e1700782. <https://doi.org/10.1126/sciadv.1700782>.
- Gao DW, Wen ZD. 2016. Phthalate esters in the environment: a critical review of their occurrence, biodegradation, and removal during wastewater treatment processes. *Sci Total Environ* 541:986–1001. <https://doi.org/10.1016/j.scitotenv.2015.09.148>.
- Fréry N, Santonen T, Porras SP, Fucic A, Leso V, Bousoumah R, Duca RC, El Yamani M, Kolossa-Gehring M, Ndaw S, Viegas S, Iavicoli I. 2020. Biomonitoring of occupational exposure to phthalates: a systematic review. *Int J Hyg Environ Health* 229:113548. <https://doi.org/10.1016/j.ijheh.2020.113548>.
- Liang DW, Zhang T, Fang HHP, He J. 2008. Phthalates biodegradation in the environment. *Appl Microbiol Biotechnol* 80:183–198. <https://doi.org/10.1007/s00253-008-1548-5>.
- Mathieu-Denoncourt J, Wallace SJ, de Solla SR, Langlois VS. 2015. Plasticizer endocrine disruption: highlighting developmental and reproductive effects in mammals and non-mammalian aquatic species. *Gen Comp Endocrinol* 219:74–88. <https://doi.org/10.1016/j.ygcen.2014.11.003>.
- Xie Z, Ebinghaus R, Temme C, Lohmann R, Caba A, Ruck W. 2007. Occurrence and air-sea exchange of phthalates in the arctic. *Environ Sci Technol* 41:4555–4560. <https://doi.org/10.1021/es0630240>.
- Mayer FL, Stalling DL, Johnson JL. 1972. Phthalate esters as environmental contaminants. *Nature* 238:411–413. <https://doi.org/10.1038/238411a0>.
- Carnevali O, Tosti L, Speciale C, Peng C, Zhu Y, Maradonna F. 2010. DEHP impairs zebrafish reproduction by affecting critical factors in oogenesis. *PLoS One* 5:e10201. <https://doi.org/10.1371/journal.pone.0010201>.
- Chikae M, Hatano Y, Ikeda R, Morita Y, Hasan Q, Tamiya E. 2004. Effects of bis(2-ethylhexyl) phthalate and benzo[a]pyrene on the embryos of Japanese medaka (*Oryzias latipes*). *Environ Toxicol Pharmacol* 16:141–145. <https://doi.org/10.1016/j.etap.2003.11.007>.
- Caldwell JC. 2012. DEHP: genotoxicity and potential carcinogenic mechanisms—a review. *Mutat Res* 751:82–157. <https://doi.org/10.1016/j.mrrev.2012.03.001>.
- Benjamin S, Pradeep S, Sarath Josh M, Kumar S, Masai E. 2015. A monograph on the remediation of hazardous phthalates. *J Hazard Mater* 298:58–72. <https://doi.org/10.1016/j.jhazmat.2015.05.004>.
- Lertsrisopon R, Soda S, Sei K, Ike M. 2009. Abiotic degradation of four phthalic acid esters in aqueous phase under natural sunlight irradiation. *J Environ Sci* 21:285–290. [https://doi.org/10.1016/S1001-0742\(08\)62265-2](https://doi.org/10.1016/S1001-0742(08)62265-2).
- Turner A, Rawling M. 2000. The behaviour of di(2-ethylhexyl) phthalate in estuaries. *Mar Chem* 68:203–217. [https://doi.org/10.1016/S0304-4203\(99\)00078-X](https://doi.org/10.1016/S0304-4203(99)00078-X).
- Fan S, Wang J, Yan Y, Wang J, Jia Y. 2018. Excellent degradation performance of a versatile phthalic acid esters-degrading bacterium and catalytic mechanism of monoalkyl phthalate hydrolase. *Int J Mol Sci* 19:2803. <https://doi.org/10.3390/ijms19092803>.
- Huang H, Zhang XY, Chen TL, Zhao YL, Xu DS, Bai YP. 2019. Biodegradation of structurally diverse phthalate esters by a newly identified esterase with catalytic activity toward di(2-ethylhexyl) phthalate. *J Agric Food Chem* 67:8548–8558. <https://doi.org/10.1021/acs.jafc.9b02655>.
- Fan S, Wang J, Li K, Yang T, Jia Y, Zhao B, Yan Y. 2018. Complete genome sequence of *Gordonia* sp. YC-JH1, a bacterium efficiently degrading a wide range of phthalic acid esters. *J Biotechnol* 279:55–60. <https://doi.org/10.1016/j.jbiotec.2018.05.009>.
- Boll M, Geiger R, Junghare M, Schink B. 2020. Microbial degradation of phthalates: biochemistry and environmental implications. *Environ Microbiol Rep* 12:3–15. <https://doi.org/10.1111/1758-2229.12787>.
- Rabus R, Wöhlbrand L, Thies D, Meyer M, Reinhold-Hurek B, Kämpfer P. 2019. *Aromatoleum* gen. nov., a novel genus accommodating the phylogenetic lineage including *Azoarcus evansii* and related species, and proposal of *Aromatoleum aromaticum* sp. nov., *Aromatoleum petrolei* sp. nov., *Aromatoleum bremense* sp. nov., *Aromatoleum toluolicum*. *Int J Syst Evol Microbiol* 69:982–997. <https://doi.org/10.1099/ijsem.0.003244>.
- Ebenau-Jehle C, Mergelsberg M, Fischer S, Brüls T, Jehmlich N, von Bergen M, Boll M. 2017. An unusual strategy for the anoxic biodegradation of phthalate. *ISME J* 11:224–236. <https://doi.org/10.1038/ismej.2016.91>.
- Junghare M, Spitteller D, Schink B. 2016. Enzymes involved in the anaerobic degradation of *ortho*-phthalate by the nitrate-reducing bacterium *Azoarcus* sp. strain PA01. *Environ Microbiol* 18:3175–3188. <https://doi.org/10.1111/1462-2920.13447>.
- Payne KA, White MD, Fisher K, Khara B, Bailey SS, Parker D, Rattray NJ, Trivedi DK, Goodacre R, Beveridge R, Barran P, Rigby SE, Scrutton NS, Hay S, Leys D. 2015. New cofactor supports  $\alpha,\beta$ -unsaturated acid decarboxylation via 1,3-dipolar cycloaddition. *Nature* 522:497–501. <https://doi.org/10.1038/nature14560>.
- Wei ST-S, Chen Y-L, Wu Y-W, Wu T-Y, Lai Y-L, Wang P-H, Ismail W, Lee T-H, Chiang Y-R. 25 March 2021. Integrated multi-omics investigations reveal the key role of synergistic microbial networks in removing plasticizer di(2-ethylhexyl) phthalate from estuarine sediments. *BioRxiv* <https://doi.org/10.1101/2021.03.24.436900>.
- White MD, Payne KA, Fisher K, Marshall SA, Parker D, Rattray NJ, Trivedi DK, Goodacre R, Rigby SE, Scrutton NS, Hay S, Leys D. 2015. UbiX is a flavin prenyltransferase required for bacterial ubiquinone biosynthesis. *Nature* 522:502–506. <https://doi.org/10.1038/nature14559>.

24. Wei STS, Wu YW, Lee TH, Huang YS, Yang CY, Chen YL, Chiang YR. 2018. Microbial functional responses to cholesterol catabolism in denitrifying sludge. *mSystems* 3:e00113-18. <https://doi.org/10.1128/mSystems.00113-18>.
25. Shih CJ, Chen YL, Wang CH, Wei STS, Lin IT, Ismail WA, Chiang YR. 2017. Biochemical mechanisms and microorganisms involved in anaerobic testosterone metabolism in estuarine sediments. *Front Microbiol* 8:1520. <https://doi.org/10.3389/fmicb.2017.01520>.
26. Yang FC, Chen YL, Tang SL, Yu CP, Wang PH, Ismail W, Wang CH, Ding JY, Yang CY, Yang CY, Chiang YR. 2016. Integrated multi-omics analyses reveal the biochemical mechanisms and phylogenetic relevance of anaerobic androgen biodegradation in the environment. *ISME J* 10:1967–1983. <https://doi.org/10.1038/ismej.2015.255>.
27. Chiang YR, Wei STS, Wang PH, Wu PH, Yu CP. 2020. Microbial degradation of steroid sex hormones: implications for environmental and ecological studies. *Microb Biotechnol* 13:926–949. <https://doi.org/10.1111/1751-7915.13504>.
28. Yuan SY, Huang IC, Chang BV. 2010. Biodegradation of dibutyl phthalate and di-(2-ethylhexyl) phthalate and microbial community changes in mangrove sediment. *J Hazard Mater* 184:826–831. <https://doi.org/10.1016/j.jhazmat.2010.08.116>.
29. Xu G, Li F, Wang Q. 2008. Occurrence and degradation characteristics of dibutyl phthalate (DBP) and di-(2-ethylhexyl) phthalate (DEHP) in typical agricultural soils of China. *Sci Total Environ* 393:333–340. <https://doi.org/10.1016/j.scitotenv.2008.01.001>.
30. Chang BV, Liao CS, Yuan SY. 2005. Anaerobic degradation of diethyl phthalate, di-*n*-butyl phthalate, and di-(2-ethylhexyl) phthalate from river sediment in Taiwan. *Chemosphere* 58:1601–1607. <https://doi.org/10.1016/j.chemosphere.2004.11.031>.
31. Louie TS, Giovannelli D, Yee N, Narasingarao P, Starovoytov V, Göker M, Klenk HP, Lang E, Kyrpides NC, Woyke T, Bini E, Häggblom MM. 2016. High-quality draft genome sequence of *Sedimenticola selenatireducens* strain AK40H1T, a gammaproteobacterium isolated from estuarine sediment. *Stand Genomic Sci* 11:66. <https://doi.org/10.1186/s40793-016-0191-5>.
32. Flood BE, Jones DS, Bailey JV. 2015. *Sedimenticola thiotaurini* sp. nov., a sulfur-oxidizing bacterium isolated from salt marsh sediments, and emended descriptions of the genus *Sedimenticola* and *Sedimenticola selenatireducens*. *Int J Syst Evol Microbiol* 65:2522–2530. <https://doi.org/10.1099/ijs.0.000295>.
33. Narasingarao P, Häggblom MM. 2006. *Sedimenticola selenatireducens*, gen. nov., sp. nov., an anaerobic selenate-respiring bacterium isolated from estuarine sediment. *Syst Appl Microbiol* 29:382–388. <https://doi.org/10.1016/j.syapm.2005.12.011>.
34. Carlström CI, Loutey DE, Wang O, Engelbrekton A, Clark I, Lucas LN, Somasekhar PY, Coates JD. 2015. Phenotypic and genotypic description of *Sedimenticola selenatireducens* strain CUZ, a marine (per)chlorate-respiring gammaproteobacterium, and its close relative the chlorate-respiring *Sedimenticola* strain NSS. *Appl Environ Microbiol* 81:2717–2726. <https://doi.org/10.1128/AEM.03606-14>.
35. Yu K, Yi S, Li B, Guo F, Peng X, Wang Z, Wu Y, Alvarez-Cohen L, Zhang T. 2019. An integrated meta-omics approach reveals substrates involved in synergistic interactions in a bisphenol A (BPA)-degrading microbial community. *Microbiome* 7:16. <https://doi.org/10.1186/s40168-019-0634-5>.
36. Geiger RA, Junghare M, Mergelsberg M, Ebenau-Jehle C, Jesenofsky VJ, Jehmlich N, von Bergen M, Schink B, Boll M. 2019. Enzymes involved in phthalate degradation in sulphate-reducing bacteria. *Environ Microbiol* 21:3601–3612. <https://doi.org/10.1111/1462-2920.14681>.
37. Zhu F, Zhu C, Zhou D, Gao J. 2019. Fate of di (2-ethylhexyl) phthalate and its impact on soil bacterial community under aerobic and anaerobic conditions. *Chemosphere* 216:84–93. <https://doi.org/10.1016/j.chemosphere.2018.10.078>.
38. Zhu F, Doyle E, Zhu C, Zhou D, Gu C, Gao J. 2020. Metagenomic analysis exploring microbial assemblages and functional genes potentially involved in di(2-ethylhexyl) phthalate degradation in soil. *Sci Total Environ* 715:137037. <https://doi.org/10.1016/j.scitotenv.2020.137037>.
39. Anantharaman K, Brown CT, Hug LA, Sharon I, Castelle CJ, Probst AJ, Thomas BC, Singh A, Wilkins MJ, Karaoz U, Brodie EL, Williams KH, Hubbard SS, Banfield JF. 2016. Thousands of microbial genomes shed light on interconnected biogeochemical processes in an aquifer system. *Nat Commun* 7:13219. <https://doi.org/10.1038/ncomms13219>.
40. Ahmad F, Zhu D, Sun J. 2020. Bacterial chemotaxis: a way forward to aromatic compounds biodegradation. *Environ Sci Eur* 32:52. <https://doi.org/10.1186/s12302-020-00329-2>.
41. Lacal J, Muñoz-Martínez F, Reyes-Darías J-A, Duque E, Matilla M, Segura A, Calvo J-JO, Jiménez-Sánchez C, Krell T, Ramos JL. 2011. Bacterial chemotaxis towards aromatic hydrocarbons in *Pseudomonas*. *Environ Microbiol* 13:1733–1744. <https://doi.org/10.1111/j.1462-2920.2011.02493.x>.
42. Parales RE, Luu RA, Hughes JG, Ditty JL. 2015. Bacterial chemotaxis to xenobiotic chemicals and naturally-occurring analogs. *Curr Opin Biotechnol* 33:318–326. <https://doi.org/10.1016/j.copbio.2015.03.017>.
43. Sanz D, García JL, Díaz E. 2020. Expanding the current knowledge and biotechnological applications of the oxygen-independent *ortho*-phthalate degradation pathway. *Environ Microbiol* 22:3478–3493. <https://doi.org/10.1111/1462-2920.15119>.
44. Kloesges T, Popa O, Martin W, Dagan T. 2011. Networks of gene sharing among 329 proteobacterial genomes reveal differences in lateral gene transfer frequency at different phylogenetic depths. *Mol Biol Evol* 28:1057–1074. <https://doi.org/10.1093/molbev/msq297>.
45. Nogales B, Lanfrancani MP, Piña-Villalonga JM, Bosch R. 2011. Anthropogenic perturbations in marine microbial communities. *FEMS Microbiol Rev* 35:275–298. <https://doi.org/10.1111/j.1574-6976.2010.00248.x>.
46. Pointing SB, Fierer N, Smith GJD, Steinberg PD, Wiedmann M. 2016. Quantifying human impact on Earth's microbiome. *Nat Microbiol* 1:16145. <https://doi.org/10.1038/nmicrobiol.2016.145>.
47. Wright RJ, Bosch R, Gibson MI, Christie-Oleza JA. 2020. Plasticizer degradation by marine bacterial isolates: a proteogenomic and metabolomic characterization. *Environ Sci Technol* 54:2244–2256. <https://doi.org/10.1021/acs.est.9b05228>.
48. Zhao HM, Hu RW, Chen XX, Bin Chen X, Lü H, Li YW, Li H, Mo CH, Cai QY, Wong MH. 2018. Biodegradation pathway of di-(2-ethylhexyl) phthalate by a novel *Rhodococcus pyridinivorans* XB and its bioaugmentation for remediation of DEHP contaminated soil. *Sci Total Environ* 640–641:1121–1131. <https://doi.org/10.1016/j.scitotenv.2018.05.334>.
49. Bhatt P, Gangola S, Bhandari G, Zhang W, Maithani D, Mishra S, Chen S. 2021. New insights into the degradation of synthetic pollutants in contaminated environments. *Chemosphere* 268:128827. <https://doi.org/10.1016/j.chemosphere.2020.128827>.
50. Yuan S, Liu C, Liao C, Chang B. 2002. Occurrence and microbial degradation of phthalate esters in Taiwan river sediments. *Chemosphere* 49:1295–1299. [https://doi.org/10.1016/s0045-6535\(02\)00495-2](https://doi.org/10.1016/s0045-6535(02)00495-2).
51. Fan LF, Shieh WY, Wu WF, Chen CP. 2006. Distribution of nitrogenous nutrients and denitrifiers strains in estuarine sediment profiles of the Tanshui River, northern Taiwan. *Estuar Coast Shelf Sci* 69:543–553. <https://doi.org/10.1016/j.ecss.2006.05.016>.
52. Klindworth A, Pruesse E, Schweer T, Peplies J, Quast C, Horn M, Glöckner FO. 2013. Evaluation of general 16S ribosomal RNA gene PCR primers for classical and next-generation sequencing-based diversity studies. *Nucleic Acids Res* 41:e1. <https://doi.org/10.1093/nar/gks808>.
53. Edgar RC. 2010. Search and clustering orders of magnitude faster than BLAST. *Bioinformatics* 26:2460–2461. <https://doi.org/10.1093/bioinformatics/btq461>.
54. Edgar RC. 2013. UPARSE: highly accurate OTU sequences from microbial amplicon reads. *Nat Methods* 10:996–998. <https://doi.org/10.1038/nmeth.2604>.
55. Quast C, Pruesse E, Yilmaz P, Gerken J, Schweer T, Yarza P, Peplies J, Glöckner FO. 2013. The SILVA ribosomal RNA gene database project: improved data processing and web-based tools. *Nucleic Acids Res* 41:D590–D596. <https://doi.org/10.1093/nar/gks1219>.
56. Schloss PD, Westcott SL, Ryabin T, Hall JR, Hartmann M, Hollister EB, Lesniewski RA, Oakley BB, Parks DH, Robinson CJ, Sahl JW, Stres B, Thallinger GG, Van Horn DJ, Weber CF. 2009. Introducing mothur: open-source, platform-independent, community-supported software for describing and comparing microbial communities. *Appl Environ Microbiol* 75:7537–7541. <https://doi.org/10.1128/AEM.01541-09>.
57. Paulson JN, Stine OC, Bravo HC, Pop M. 2013. Differential abundance analysis for microbial marker-gene surveys. *Nat Methods* 10:1200–1202. <https://doi.org/10.1038/nmeth.2658>.
58. Chong J, Liu P, Zhou G, Xia J. 2020. Using MicrobiomeAnalyst for comprehensive statistical, functional, and meta-analysis of microbiome data. *Nat Protoc* 15:799–821. <https://doi.org/10.1038/s41596-019-0264-1>.
59. Edgar RC. 2004. MUSCLE: multiple sequence alignment with high accuracy and high throughput. *Nucleic Acids Res* 32:1792–1797. <https://doi.org/10.1093/nar/gkh340>.
60. Chong J, Soufan O, Li C, Caraus I, Li S, Bourque G, Wishart DS, Xia J. 2018. MetaboAnalyst 4.0: towards more transparent and integrative metabolomics analysis. *Nucleic Acids Res* 46:W486–W494. <https://doi.org/10.1093/nar/gky310>.



61. Bolger AM, Lohse M, Usadel B. 2014. Trimmomatic: a flexible trimmer for Illumina sequence data. *Bioinformatics* 30:2114–2120. <https://doi.org/10.1093/bioinformatics/btu170>.
62. Li D, Liu CM, Luo R, Sadakane K, Lam TW. 2015. MEGAHIT: an ultra-fast single-node solution for large and complex metagenomics assembly via succinct de Bruijn graph. *Bioinformatics* 31:1674–1676. <https://doi.org/10.1093/bioinformatics/btv033>.
63. Hyatt D, Chen G-L, LoCascio PF, Land ML, Larimer FW, Hauser LJ. 2010. Prodigal: prokaryotic gene recognition and translation initiation site identification. *BMC Bioinformatics* 11:119. <https://doi.org/10.1186/1471-2105-11-119>.
64. Wu YW, Simmons BA, Singer SW. 2016. MaxBin 2.0: an automated binning algorithm to recover genomes from multiple metagenomic datasets. *Bioinformatics* 32:605–607. <https://doi.org/10.1093/bioinformatics/btv638>.
65. Buchfink B, Xie C, Huson DH. 2015. Fast and sensitive protein alignment using DIAMOND. *Nat Methods* 12:59–60. <https://doi.org/10.1038/nmeth.3176>.
66. Parks DH, Imelfort M, Skennerton CT, Hugenholtz P, Tyson GW. 2015. CheckM: assessing the quality of microbial genomes recovered from isolates, single cells, and metagenomes. *Genome Res* 25:1043–1055. <https://doi.org/10.1101/gr.186072.114>.
67. Gurevich A, Saveliev V, Vyahhi N, Tesler G. 2013. QUAST: quality assessment tool for genome assemblies. *Bioinformatics* 29:1072–1075. <https://doi.org/10.1093/bioinformatics/btt086>.
68. Langmead B, Salzberg SL. 2012. Fast gapped-read alignment with Bowtie 2. *Nat Methods* 9:357–359. <https://doi.org/10.1038/nmeth.1923>.
69. Robinson MD, McCarthy DJ, Smyth GK. 2010. edgeR: a Bioconductor package for differential expression analysis of digital gene expression data. *Bioinformatics* 26:139–140. <https://doi.org/10.1093/bioinformatics/btp616>.
70. Hara H, Stewart GR, Mohn WW. 2010. Involvement of a novel ABC transporter and monoalkyl phthalate ester hydrolase in phthalate ester catabolism by *Rhodococcus jostii* RHA1. *Appl Environ Microbiol* 76:1516–1523. <https://doi.org/10.1128/AEM.02621-09>.
71. Mitchell AL, Attwood TK, Babbitt PC, Blum M, Bork P, Bridge A, Brown SD, Chang H-Y, El-Gebali S, Fraser MI, Gough J, Haft DR, Huang H, Letunic I, Lopez R, Luciani A, Madeira F, Marchler-Bauer A, Mi H, Natale DA, Necci M, Nuka G, Orengo C, Pandurangan AP, Paysan-Lafosse T, Pesseat S, Potter SC, Qureshi MA, Rawlings ND, Redaschi N, Richardson LJ, Rivoire C, Salazar GA, Sangrador-Vegas A, Sigrist CJA, Sillitoe I, Sutton GG, Thanki N, Thomas PD, Tosatto SCE, Yong S-Y, Finn RD. 2019. InterPro in 2019: improving coverage, classification and access to protein sequence annotations. *Nucleic Acids Res* 47:D351–D360. <https://doi.org/10.1093/nar/gky1100>.
72. Almagro Armenteros JJ, Tsirigos KD, Sønderby CK, Petersen TN, Winther O, Brunak S, von Heijne G, Nielsen H. 2019. SignalP 5.0 improves signal peptide predictions using deep neural networks. *Nat Biotechnol* 37:420–423. <https://doi.org/10.1038/s41587-019-0036-z>.
73. Pruitt KD, Tatusova T, Maglott DR. 2007. NCBI reference sequences (RefSeq): a curated non-redundant sequence database of genomes, transcripts and proteins. *Nucleic Acids Res* 35:D61–D65. <https://doi.org/10.1093/nar/gkl842>.
74. Huerta-Cepas J, Szklarczyk D, Heller D, Hernández-Plaza A, Forslund SK, Cook H, Mende DR, Letunic I, Rattai T, Jensen LJ, von Mering C, Bork P. 2019. eggNOG 5.0: a hierarchical, functionally and phylogenetically annotated orthology resource based on 5090 organisms and 2502 viruses. *Nucleic Acids Res* 47:D309–D314. <https://doi.org/10.1093/nar/gky1085>.
75. Aramaki T, Blanc-Mathieu R, Endo H, Ohkubo K, Kanehisa M, Goto S, Ogata H. 2020. KofamKOALA: KEGG ortholog assignment based on profile HMM and adaptive score threshold. *Bioinformatics* 36:2251–2252. <https://doi.org/10.1093/bioinformatics/btz859>.
76. Kumar S, Stecher G, Li M, Niyaz C, Tamura K. 2018. MEGA X: molecular evolutionary genetics analysis across computing platforms. *Mol Biol Evol* 35:1547–1549. <https://doi.org/10.1093/molbev/msy096>.
77. Junghare M, Spittler D, Schink B. 2019. Anaerobic degradation of xenobiotic isophthalate by the fermenting bacterium *Syntrophorhabdus aromaticivorans*. *ISME J* 13:1252–1268. <https://doi.org/10.1038/s41396-019-0348-5>.
78. Nahurira R, Ren L, Song J, Jia Y, Wang J, Fan S, Wang H, Yan Y. 2017. Degradation of di(2-ethylhexyl) phthalate by a novel *Gordonia alkanivorans* strain YC-RL2. *Curr Microbiol* 74:309–319. <https://doi.org/10.1007/s00284-016-1159-9>.
79. Iwata M, Imaoka T, Nishiyama T, Fujii T. 2016. Re-characterization of mono-2-ethylhexyl phthalate hydrolase belonging to the serine hydrolase family. *J Biosci Bioeng* 122:140–145. <https://doi.org/10.1016/j.jbiosc.2016.01.008>.
80. Nishioka T, Iwata M, Imaoka T, Mutoh M, Egashira Y, Nishiyama T, Shin T, Fujii T. 2006. A mono-2-ethylhexyl phthalate hydrolase from a *Gordonia* sp. that is able to dissimilate di-2-ethylhexyl phthalate. *Appl Environ Microbiol* 72:2394–2399. <https://doi.org/10.1128/AEM.72.4.2394-2399.2006>.
81. Hong DK, Jang SH, Lee CW. 2016. Gene cloning and characterization of a psychrophilic phthalate esterase with organic solvent tolerance from an Arctic bacterium *Sphingomonas glacialis* PAMC 26605. *J Mol Catal B Enzym* 133:S337–S345. <https://doi.org/10.1016/j.molcatb.2017.02.004>.
82. Whangsuk W, Sungkeeree P, Nakasiri M, Thiengmag S, Mongkolsuk S, Loprasert S. 2015. Two endocrine disrupting dibutyl phthalate degrading esterases and their compensatory gene expression in *Sphingobium* sp. SM42. *Int Biodeterior Biodegradation* 99:45–54. <https://doi.org/10.1016/j.ibiod.2014.12.006>.
83. Zhang XY, Fan X, Qiu YJ, Li CY, Xing S, Zheng YT, Xu JH. 2014. Newly identified thermostable esterase from *Sulfobacillus acidophilus*: properties and performance in phthalate ester degradation. *Appl Environ Microbiol* 80:6870–6878. <https://doi.org/10.1128/AEM.02072-14>.
84. Wu J, Liao X, Yu F, Wei Z, Yang L. 2013. Cloning of a dibutyl phthalate hydrolase gene from *Acinetobacter* sp. strain M673 and functional analysis of its expression product in *Escherichia coli*. *Appl Microbiol Biotechnol* 97:2483–2491. <https://doi.org/10.1007/s00253-012-4232-8>.
85. Jiao Y, Chen X, Wang X, Liao X, Xiao L, Miao A, Wu J, Yang L. 2013. Identification and characterization of a cold-active phthalate esters hydrolase by screening a metagenomic library derived from biofilms of a wastewater treatment plant. *PLoS One* 8:e75977. <https://doi.org/10.1371/journal.pone.0075977>.